Closed-loop Recycling of Vinylogous Urethane Vitrimers

Youwei Ma,[a,b] Xuesong Jiang,[b] Zixing Shi,[b]* José Augusto Berrocal,[a]* Christoph Weder[a]*

[a] Adolphe Merkle Institute, University of Fribourg, Chemin des Verdiers 4, CH-1700 Fribourg, Switzerland

[b] School of Chemistry and Chemical Engineering, Frontiers Science Center for Transformative Molecules, State Key Laboratory for Metal Matrix Composite Materials, Shanghai Jiao Tong University, Shanghai 200240, P. R. China

Table of Contents

Materials and Instrumentation

Materials

Poly(ethylene glycol) (**PEG**, M_n = 1000, 2000, 3000, 10000, 35000 g mol^{-1}), Polytetrahydrofuran (**PTHF**, M_n = 2000 g mol^{-1}), Tris(2-aminoethyl)amine (96%, **TREN**), *tert*-butyl acetoacetate (98%), N,N-dimethylformamide (99.8%, **DMF**), chloroform-*d* (99.8%, **CDCl₃**), deuterium oxide (**D₂O**), multi-walled carbon nanotubes (98%, **MCNs**), triethylamine (99.5%, **TEA**), strongly acidic ion exchange resin (50 to 100 mesh, DOWEX 50WX8-10) were purchased from Sigma-Aldrich.

Instrumentation

Nuclear magnetic resonance (NMR) spectroscopy. NMR spectroscopy was carried out at 297.2 K on a Bruker Avance DPX 400 spectrometer at frequencies of 400.19 MHz for ^1H nuclei. Spectra were calibrated to the residual solvent peak of CDCl$_3$ (7.26 ppm ^1H NMR), D$_2$O (4.79 ppm, ^1H NMR). Data were evaluated with the MestReNova software suite (v 12.0) and all chemical shifts (δ) are reported in parts per million (ppm) relative to tetramethylsilane with coupling constant (*J*) in Hz (multiplicity: s = singlet, d = doublet, dd = double doublet, t = triplet, m = multiplet, br = broad signal).

Fourier Transform Infrared Spectroscopy (FTIR). FTIR was carried out on a Bruker Tensor 27 spectrometer. Samples were analysed in attenuated total reflectance (ATR) mode using a diamond crystal.

Differential scanning calorimetry (DSC) measurements were performed under a nitrogen atmosphere using a Mettler-Toledo STAR system operating at a heating/cooling rate of 10 °C min^{-1} in the temperature range of -20 to 100 °C using a sample mass of ca. 5 mg, unless indicated otherwise. The melting temperature, T_m, is reported based on the minimum of the major endothermic melting peak.

Dynamic mechanical analyses (DMA) were performed on the TA Instrument Model Q800 in tension mode. The temperature ranged from -20 to 100 °C with a heating rate of 3 °C min^{-1}, a frequency of 1Hz, and an amplitude of 0.5% strain.

Stress relaxation analyses were carried out on the TA Instrument Model Q800 in tension mode. In the test, a rectangular sample was first kept isothermally at a specific temperature for 3 min. Then a constant 1% strain was applied to the sample and the stress was recorded at the same

time.

Tensile testing. Unless stated otherwise, stress-strain measurements were carried out at 100 mm·min^{-1} with a Zwick/Roell Z010 tensile tester equipped with a 200 N load cell. Uniaxial tensile tests were carried out with dog-bone-shaped samples with dimensions of $40 \times 5 \times 0.2$ mm (length $\times$ width $\times$ thickness) that were cut from compression molded films according to ASTM D1708. The testing procedure followed the standard method described in ASTM D1708.

Solubility experiment. The weighed samples ($M_{initial}$) were immersed in DMF and shaked in a shaking bed for 24 h. The DMF was changed every 6 h. The solvent was carefully removed with a syringe, and the surface was wiped with a tissue after swelling, after which the samples were weighed ($M_{swelling}$). The samples were dried under vacuum at 80 °C for 24 h to ensure complete removal of the solvent from the material. After drying, the samples were weighed again (M_{drying}). The swelling ratio was defined as $M_{swelling}/M_{initial}$, whereas the gel fraction was defined as $M_{drying}/M_{initial}$.

Compression testing. Compression tests were performed with a Carver 3851-0 press. The samples were cut into small pieces using scissors. The pieces were piled up and placed between two sheets of Teflon, compressed between two plates of steel at a distance of 0.2 mm, applying a pressure of 10 MPa for 30 min at 150 °C.

Scanning Electron Microscopy (SEM) and Raman spectroscopy. The morphology and structure of the multi-walled carbon nanotubes before and after depolymerization of the vinylogous urethane vitrimer were analyzed by a SEM instrument equipped with a Rise-magna™ Raman spectrophotometer (TESCAN, Czech Republic).

Synthesis and Characterization

Synthesis of poly(ethylene glycol) bisacetoacetate (aPEGx)

n = 20 43 65 225 793
x = 1k 2k 3k 10k 35k
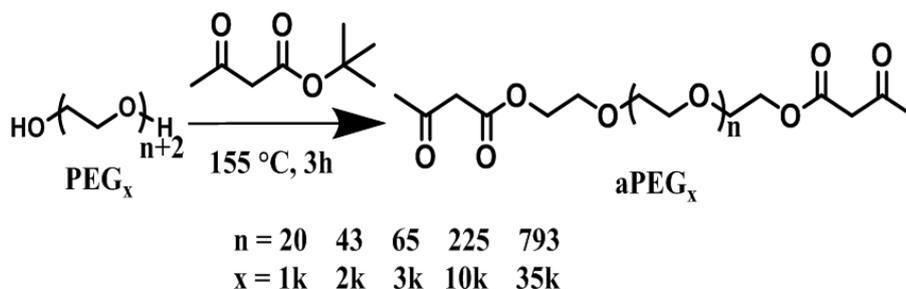
Compounds from the **aPEGx** series were all prepared adapting a literature procedure.[18] Commercial **PEGx** (20 g, **x** = 1000, 2000, 3000, 10000, 35000 g mol^{-1}) was weighed and added into a 250 mL single-necked flask, together with a stirring bar. The flask was equipped with a condenser and a Dean-Stark apparatus to remove the *tert*-butanol generated during the reaction. Then, *tert*-butyl acetoacetate (20 eq. for **x** < 10000 g·mol^{-1}; 50 eq. for **x** = 10000, 35000 g·mol^{-1}) was added in one portion with a pipette, and the resulting mixture was heated at 155 °C for 3 h. A crude product was obtained via precipitation by adding the mixture in 200 mL of hexane. The precipitate was washed three times to obtain the final poly(ethylene glycol) bisacetoacetate (**aPEGx**). The extent of end-group functionalization was determined by integration of the ^{1}H NMR signals following the equation:

Conversion rate = (n × 2)/Integration of peak 3 × 100

aPEG$_{1k}$: yield 93.8 %, 21.9 g. ^{1}H NMR (400 MHz, Chloroform-*d*) δ 4.32 – 4.26 (m, 2H), 3.73 – 3.68 (m, 2H), 3.63 (d, J = 1.0 Hz, 40H), 3.48 (s, 2H), 2.27 (s, 3H).

The conversion was estimated from the ^{1}H NMR spectrum in Figure S1: (20 × 2)/39.3×100 ≈ 100.0 %.

aPEG$_{2k}$: yield 90.0 %, 19.5 g. ^{1}H NMR (400 MHz, Chloroform-*d*) δ 4.33 – 4.30 (m, 2H), 3.74 – 3.71 (m, 2H), 3.66 (d, J = 1.1 Hz, 93H), 3.50 (s, 2H), 2.29 (s, 3H).

The conversion was estimated from the ^{1}H NMR spectrum in Figure S2: (43 × 2)/93.4 × 100 = 92.0 %.

aPEG$_{3k}$: yield 89.5%, 18.9 g. ^{1}H NMR (400 MHz, Chloroform-*d*) δ 4.34 – 4.28 (m, 2H), 3.74 – 3.71 (m, 2H), 3.65 (s, 130H), 3.49 (s, 2H), 2.28 (s, 3H).

The conversion was estimated from the ^{1}H NMR spectrum in Figure S3: $(65 \times 2)/130.5 \times 100 = 99.6\%$

aPEG$_{10k}$: yield 91.6 %, 18.6 g. ^{1}H NMR (400 MHz, Chloroform-*d*) δ 4.35 – 4.29 (m, 2H), 3.75 – 3.72 (m, 2H), 3.66 (s, 452H), 3.49 – 3.47 (m, 2H), 2.29 (s, 3H).

The conversion was estimated from the ^{1}H NMR spectrum in Figure S4: $(225 \times 2)/452.3 \times 100 \approx 99.5\%$.

aPEG$_{35k}$: yield 92.3 %, 18.5 g. ^{1}H NMR (500 MHz, Chloroform-*d*) δ 4.32 (t, J = 1.6 Hz, 2H), 3.73 (s, 2H), 3.66 (s, 1632H), 3.52 (d, J = 0.9 Hz, 2H), 2.30 (s, 3H).

The conversion was estimated from the ^{1}H NMR spectrum in Figure S5: $(793 \times 2)/1632 \times 100 = 97.2\%$.

Synthesis of polytetrahydrofuran bisacetoacetate (aPTHF$_{2k}$)
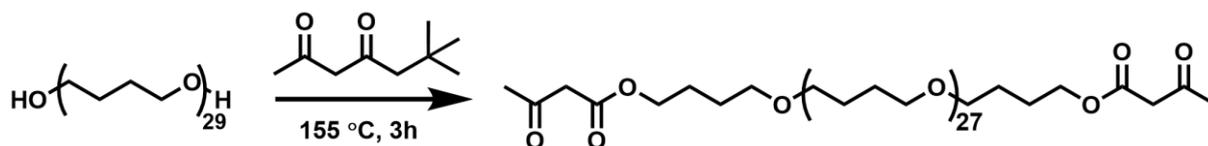
Commercial **PTHF$_{2k}$** (6 g, **x** = 2000 g mol^{-1}) was weighed and added into a 50 mL single-necked flask, together with a stirring bar. The flask was equipped with a condenser and a Dean-Stark apparatus to remove the *tert*-butanol generated during the reaction. Then, *tert*-butyl acetoacetate (9.5 g) was added in one portion with a pipette, and the resulting mixture was heated at 155 °C for 3 h. The unreated *tert*-butyl acetoacetate was removed by vacuum distillation at 100 °C for 12 h to afford polytetrahydrofuran bisacetoacetate (**aPTHF$_{2k}$**). The extent of end-group functionalization was determined by integration of the ^{1}H NMR signals in Figure S6 following the equation:

Conversion rate = (27×2)/Integration of peak $5 \times 100 = 54/58 \times 100 = 93.1\%$

aPTHF$_{2k}$: yield 97%, 6.4 g. ^{1}H NMR (400 MHz, CDCl$_3$) δ 4.10 (t, J = 6.6 Hz, 2H), 3.38 (s, 2H), 3.38 – 3.32 (m, 58H), 2.20 (s, 3H), 1.55 (h, J = 3.0 Hz, 58H).
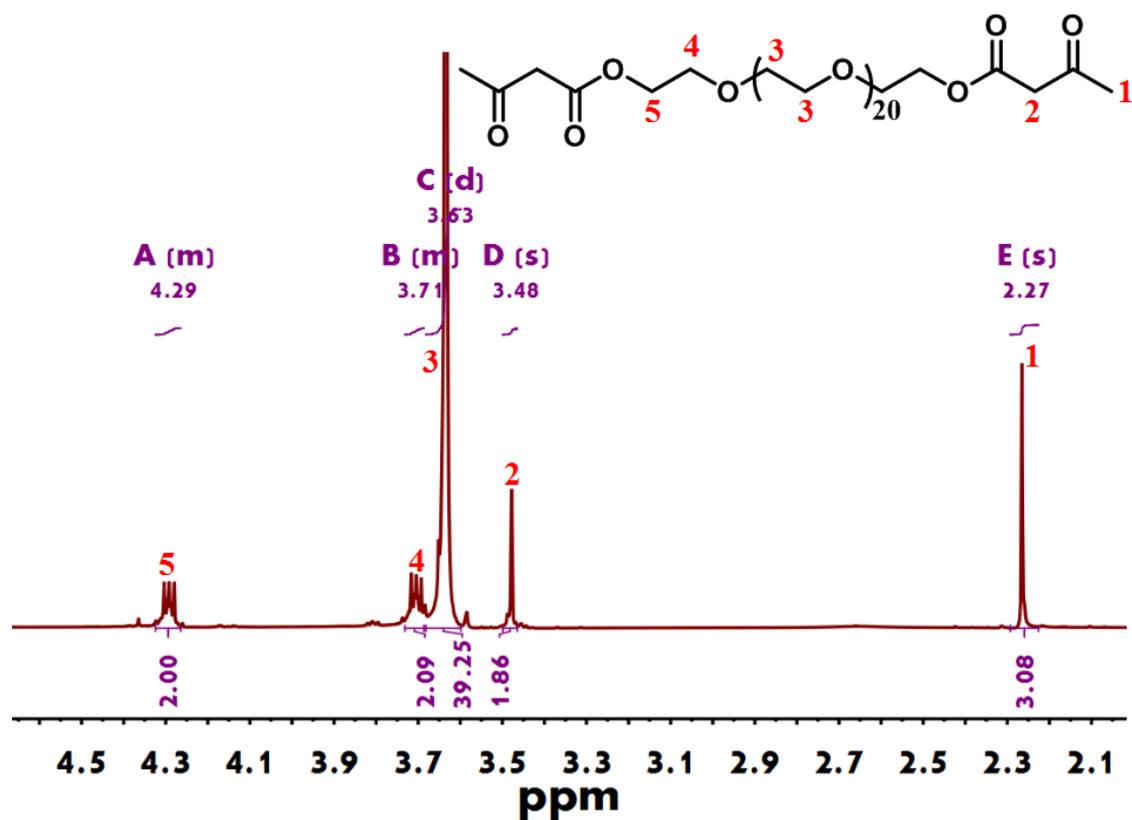
Figure S1. ^{1}H NMR spectrum (CDCl$_3$, 400 MHz) of **aPEG$_{1k}$**.
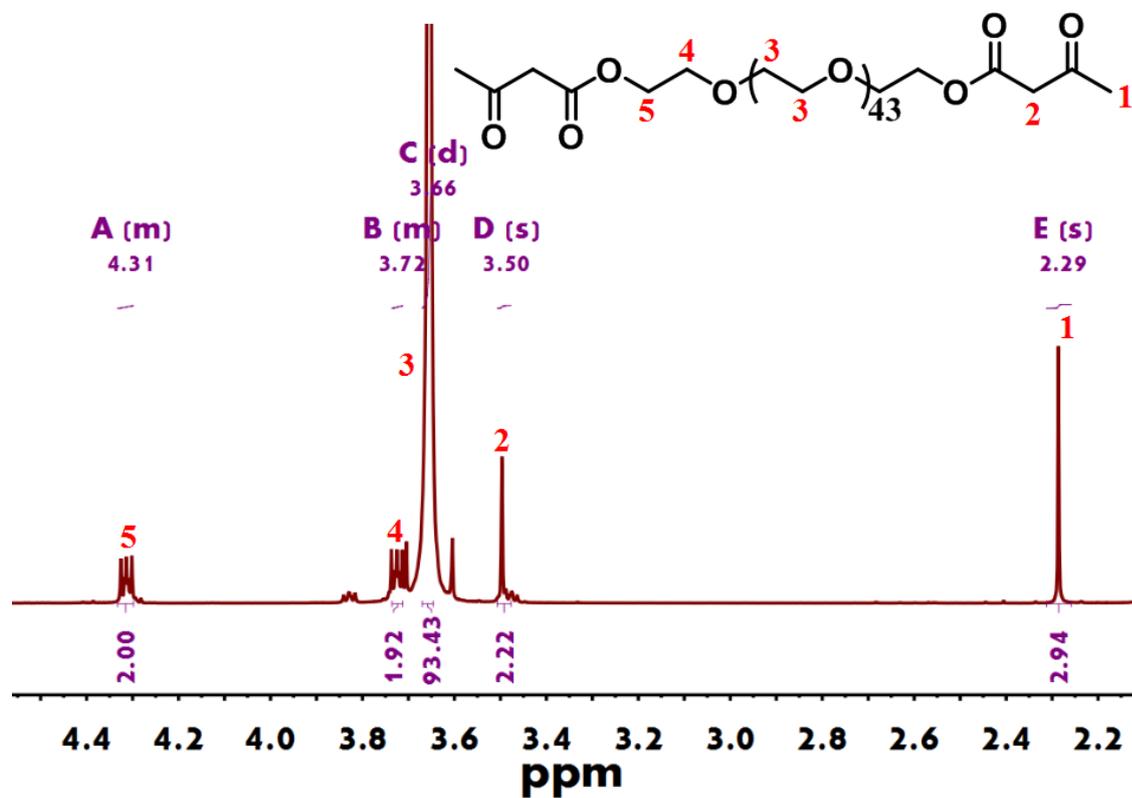
Figure S2. ^{1}H NMR spectrum (CDCl$_3$, 400 MHz) of **aPEG$_{2k}$**.
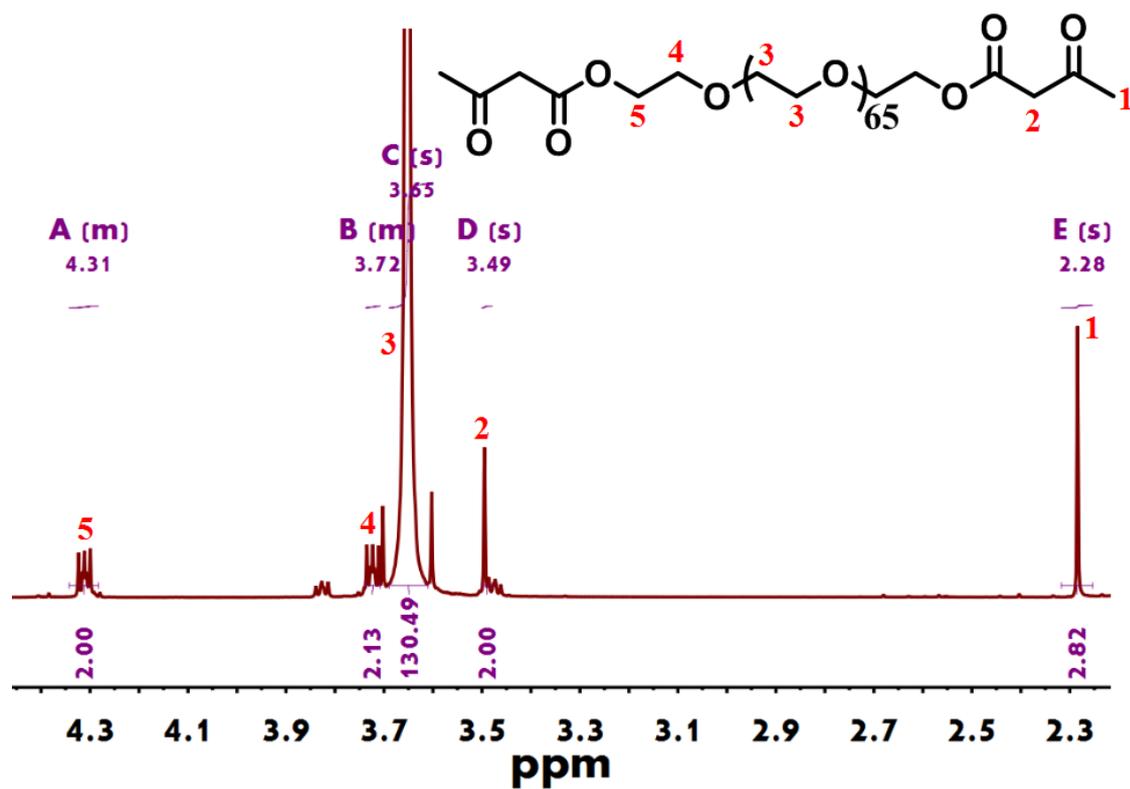
Figure S3. ^{1}H NMR spectrum (CDCl$_3$, 400 MHz) of **aPEG$_{3k}$**.
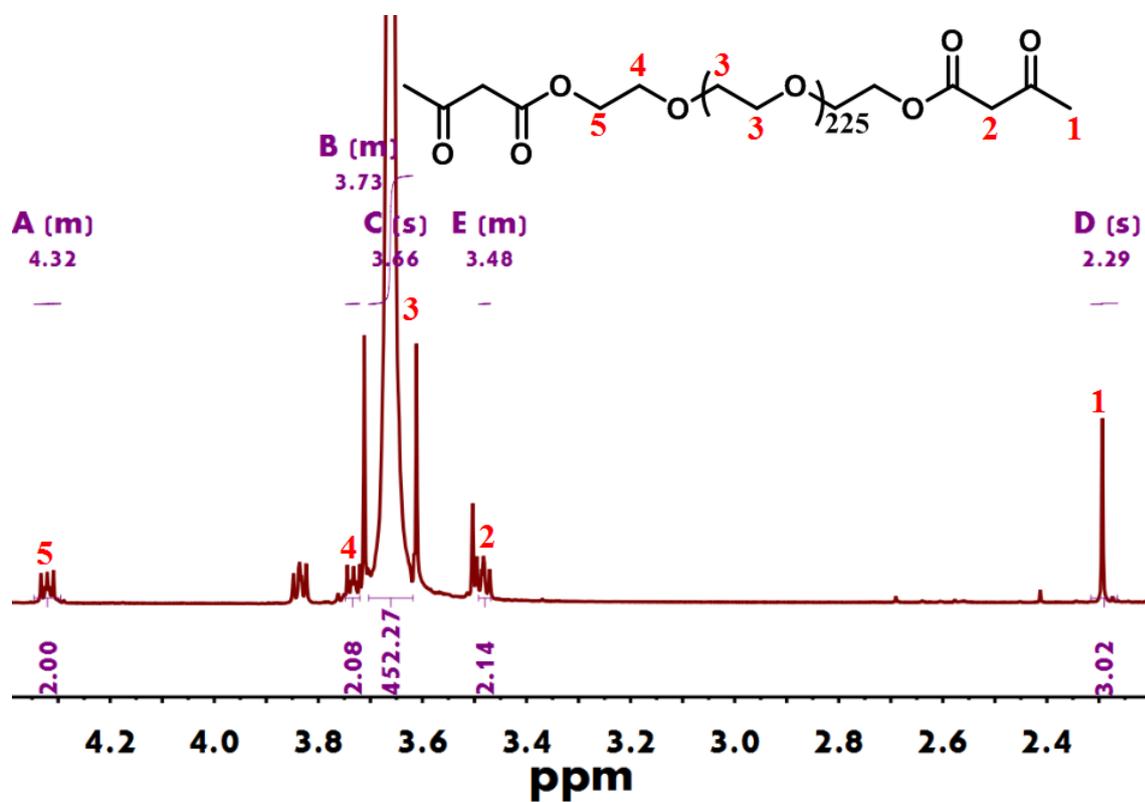
Figure S4. ^{1}H NMR spectrum (CDCl$_3$, 400 MHz) of **aPEG$_{10k}$**.
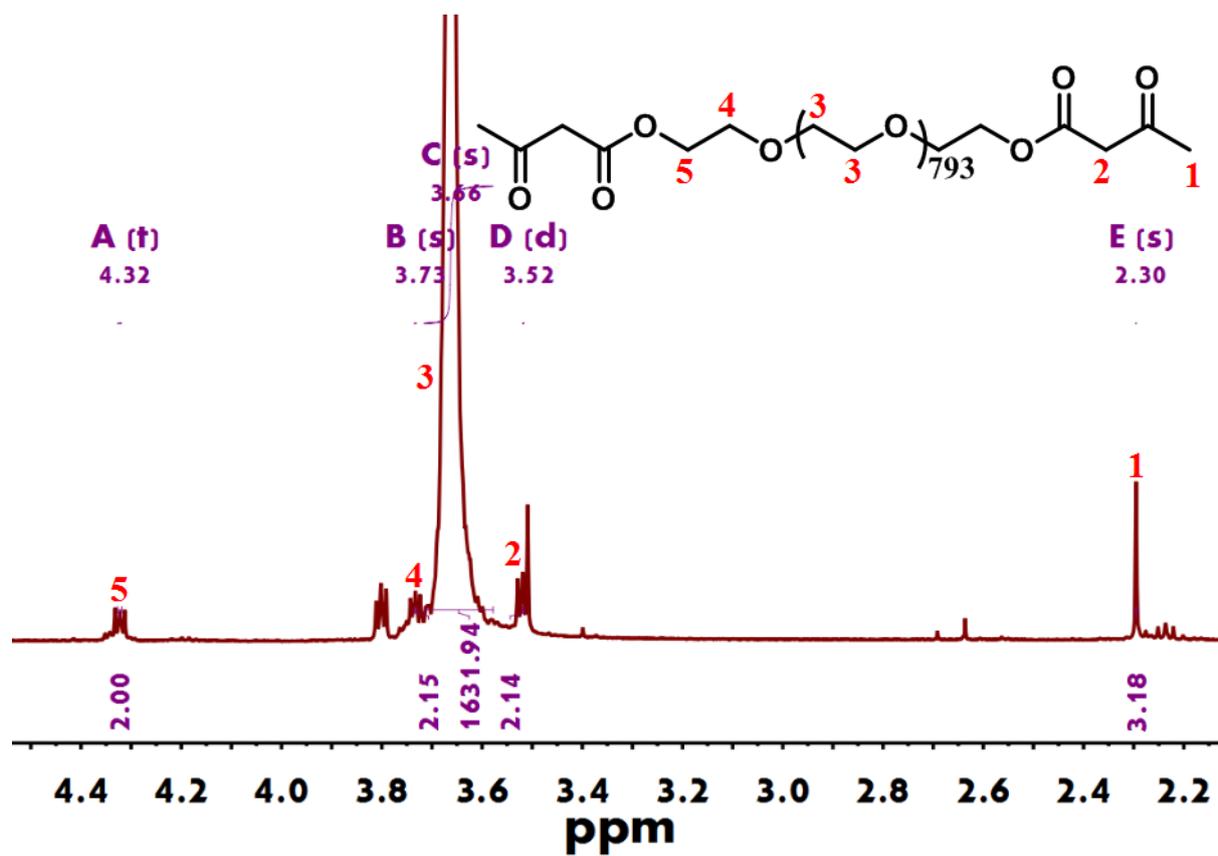
Figure S5. ^{1}H NMR spectrum (CDCl$_3$, 400 MHz) of **aPEG$_{35k}$**.
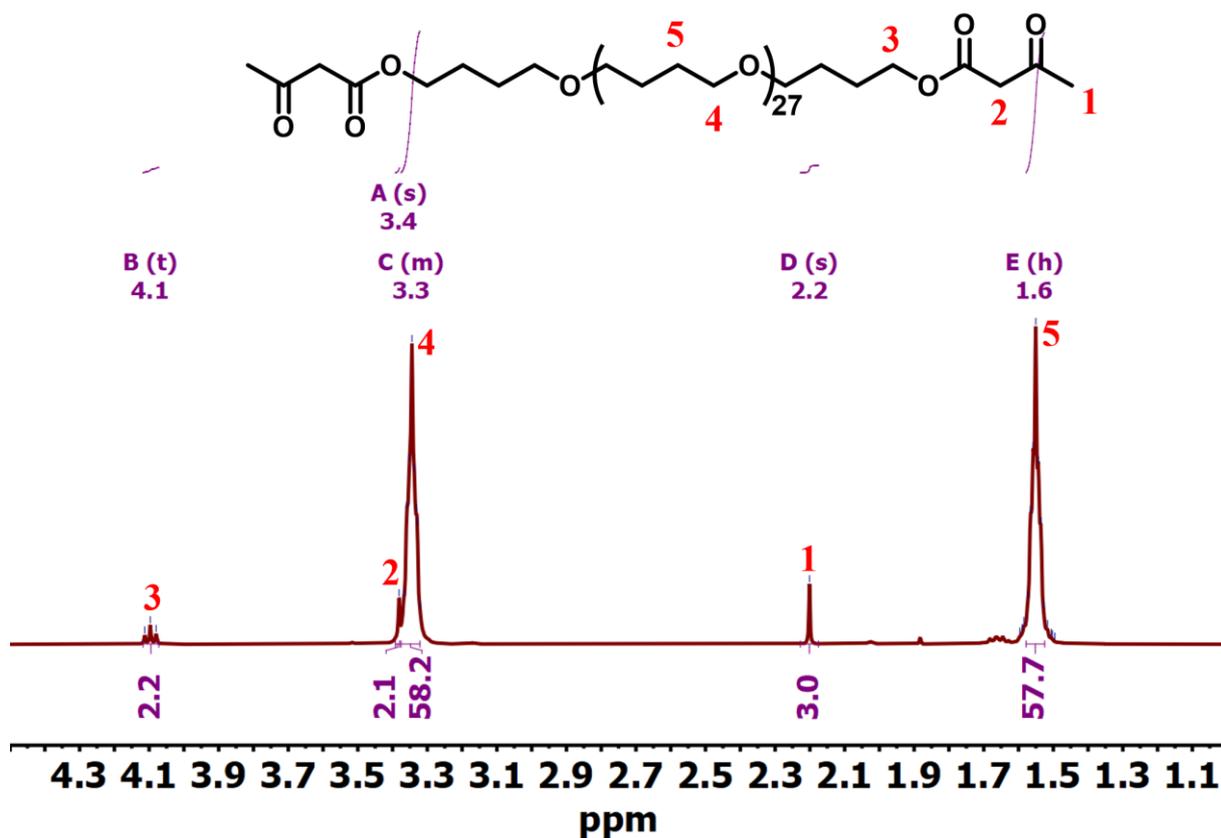

Figure S6. ^{1}H NMR spectrum (CDCl$_3$, 400 MHz) of **aPTHF$_{2k}$**.

**Synthesis of vinylogous urethane vitrimers**
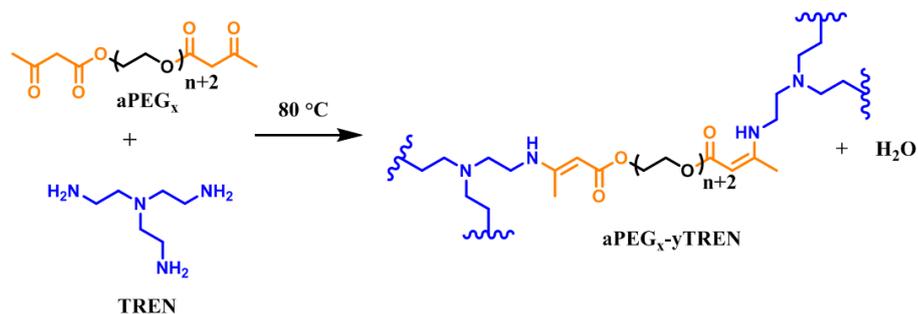
Figure S7. Synthesis of **aPEG$_x$-yTREN**.

In a typical procedure to synthesize the VU vitrimer, **aPEG$_x$** (1.2 g for **aPEG$_{1k}$**, 2.2 g for **aPEG$_{2k}$**, 3.2 g for **aPEG$_{3k}$**, 1.02 g for **aPEG$_{10k}$**, 3.52 g for **aPEG$_{35k}$**; ~1 mmol for **aPEG$_{1k, 2k, 3k}$**, ~0.1 mmol for **aPEG$_{10k, 35k}$**) was dissolved in 5-10 mL of DMF in a 10 mL vial (gently heating by heat gun allows to speed up the dissolution process). Then, **TREN** was added to the mixture (reaction scheme shown in Figure S7). The resulting solution was stirred for 10 min at room temperature, and then poured into a Teflon mold. The mixture was heated at 80 °C overnight in a drying oven (no vacuum), and then it was dried by applying vacuum at 80 °C for 12 h. A brownish solid was obtained, which was labeled as **aPEG$_x$-yTREN**. Vitrimers from the reaction of **aPEG$_{2k}$** and different amounts of excess amine (0, 20, and 50 mol%) were prepared by adjusting the molar ratio of **TREN** added. The specific amounts used for the preparation of the **aPEG$_x$-yTREN** library are reported in Table S1.

Table S1. Amount of **aPEG$_x$** and **TREN** used in the synthesis of **aPEG$_x$-yTREN**.

Sample name	aPEG$_x$		TREN	
	Weight (g)	mmol	Weight (g)	mmol
aPEG$_{1k}$-1.2TREN	1.2	1	0.117	0.8
aPEG$_{2k}$-1.2TREN	2.2	1	0.117	0.8
aPEG$_{3k}$-1.2TREN	3.2	1	0.117	0.8
aPEG$_{10k}$-1.2TREN	1.02	0.1	0.012	0.08
aPEG$_{35k}$-1.2TREN	3.52	0.1	0.012	0.08
aPEG$_{2k}$-1.0TREN	2.2	1	0.098	0.67
aPEG$_{2k}$-1.5TREN	2.2	1	0.146	1
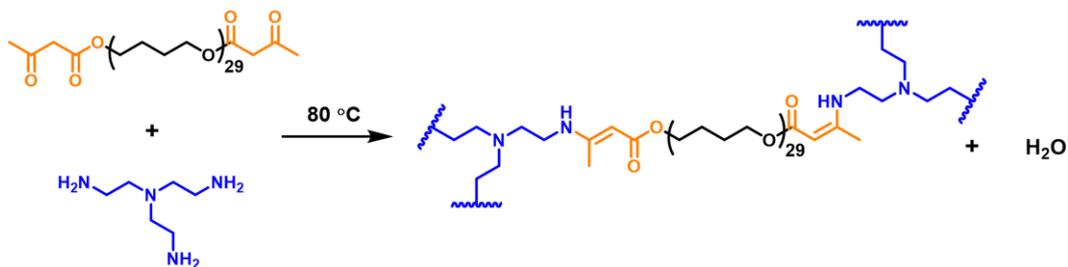
Figure S8. Synthesis of **aPTHF$_{2k}$ -1.2TREN**.

To synthesize the **aPTHF$_{2k}$**-based **VU** vitrimer, a procedure similar to the one employed for **aPEG$_x$-yTREN** was used. **aPTHF$_{2k}$** (4.4 g) was dissolved in 10 mL of ethanol in a 20 mL vial. Then, **TREN** (0.257 g) was added to the mixture (reaction scheme shown in Figure S8). The resulting solution was stirred for 10 min at room temperature and then poured into a Teflon mold. The mixture was left at room temperature over night (no vacuum), and then it was dried by vacuum oven at 80 °C for 24 h. A brownish solid was obtained, which was labeled as **aPTHF$_{2k}$ -1.2TREN**.
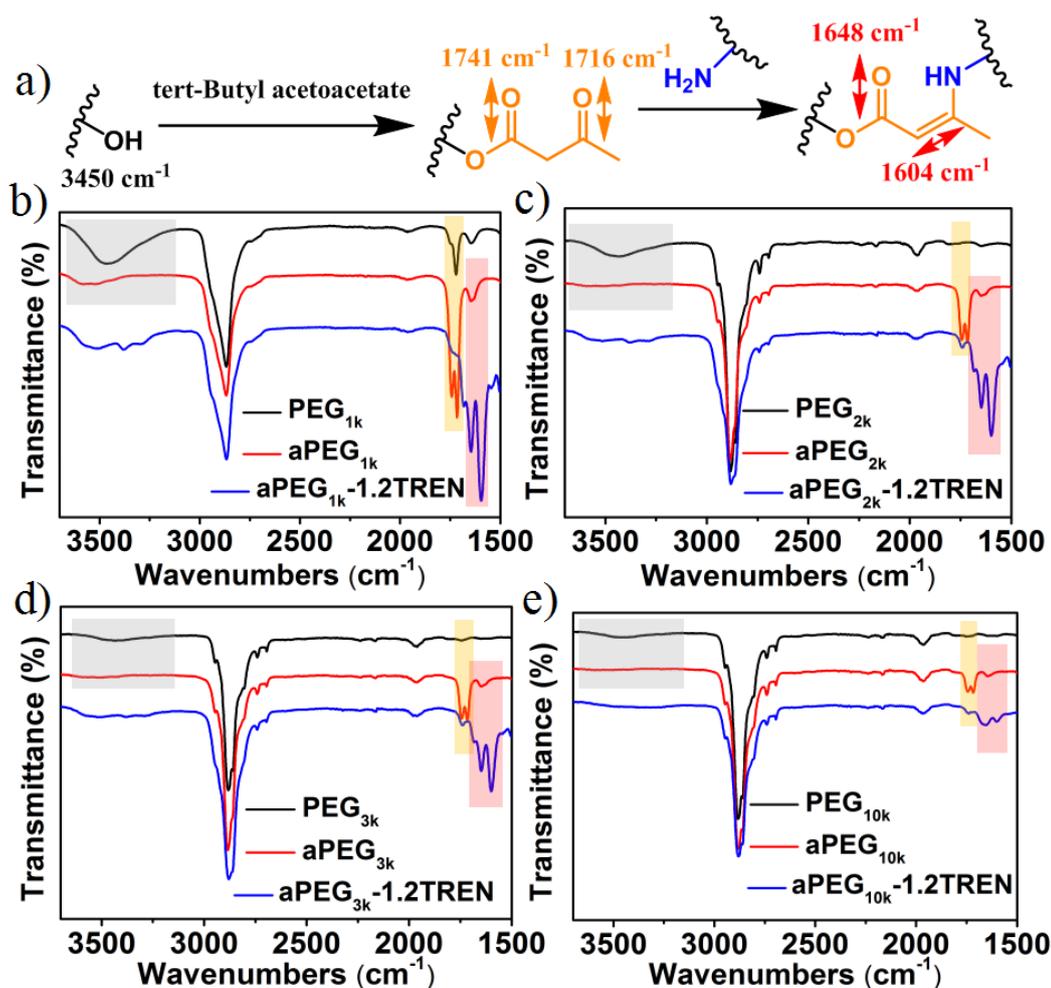
Figure S9. Synthesis of vinylogous urethanes from **PEG$_x$** (a). FTIR spectra (b-e) showing the conversion of the starting **PEG$_x$** (black line) into the corresponding **aPEG$_x$** (red line), and then into **aPEG$_x$-1.2TREN** (blue line) for **x** = 1k (b), 2k (c), 3k (d), 10k (e). The grey areas highlight the spectrum region of the *-OH* stretching vibrations (around 3450 cm^{-1}), before and after the acetylacetylation of **PEG$_x$**. The yellow areas highlight the spectrum region of carbonyl stretching vibrations (1716 cm^{-1}, 1741 cm^{-1}). The pink areas highlight the spectrum region associated to the stretching vibrations of the carbonyl groups (1648 cm^{-1}) and double bonds (1604 cm^{-1}).
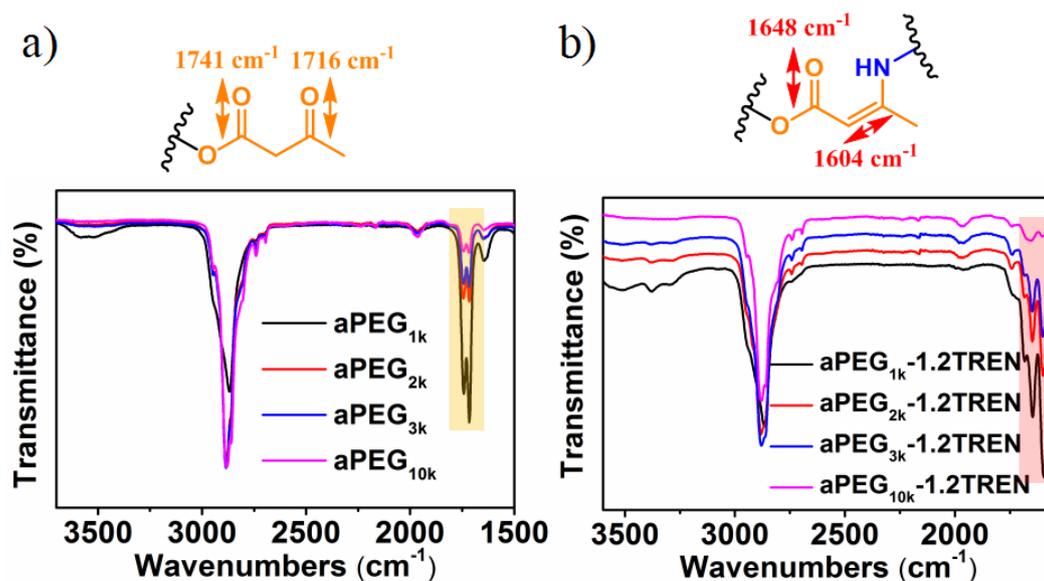
Figure S10. Assignment of the characteristic bands of the acetoacetyl moieties (1716, 1741 cm^{-1}) in the FTIR spectra of **aPEG$_x$**, with **x** = 1k, 2k, 3k, 10k (a). The yellow area highlights the characteristic bands of the acetoacetyl groups (1716, 1741 cm^{-1}), and the decrease in the intensity of such signals upon increasing the molecular weight of **aPEG$_x$**. Assignment of the characteristic bands of the vinylogous urethane groups (1604, 1648 cm^{-1}) in the FTIR spectra of **aPEG$_x$-1.2TREN** (b). The red area highlights the characteristic bands of the vinylogous urethane moiety (1604, 1648 cm^{-1}), and the decrease in the intensity of such signals upon increasing the molecular weight of **aPEG$_x$**.
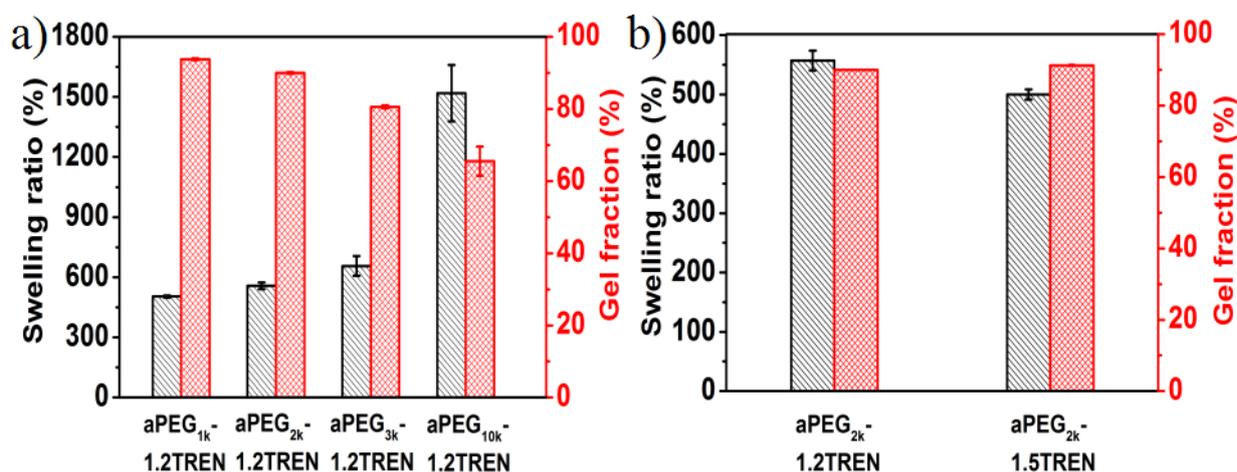
Figure S11. Swelling ratio (grey) and gel fraction (red) of (a) **aPEG$_x$-1.2TREN** and (b) **aPEG$_{2k}$-yTREN**. **aPEG$_{2k}$-1.0TREN** and **aPEG$_{35k}$-1.2TREN** completely dissolved in DMF and hence could not be measured.
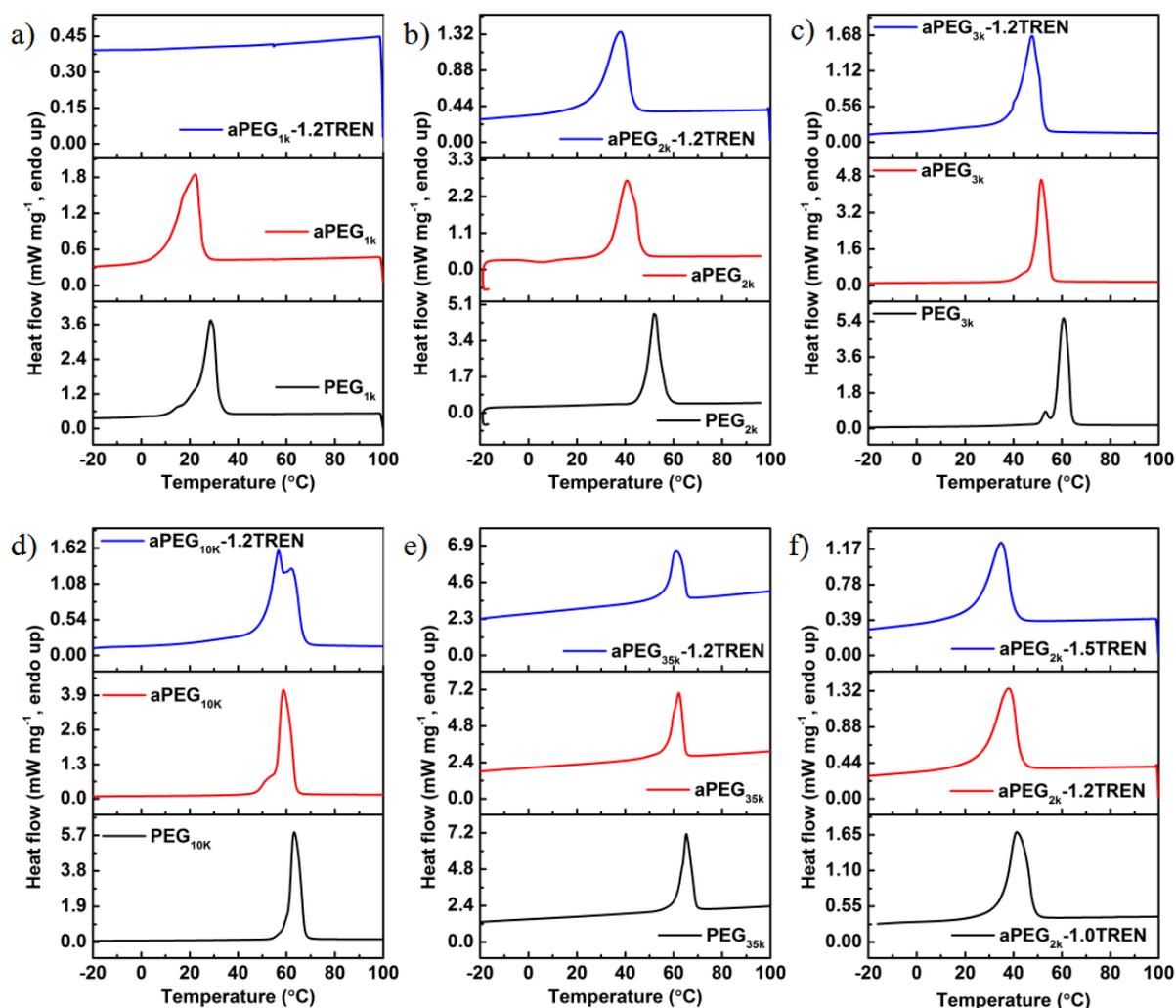
Figure S12. DSC traces of the second heating runs for **PEGx** (black line), **aPEGx** (red line), **aPEGx-1.2TREN** (blue line) with   **x** = 1k (a), 2k (b), 3k (c), 10k (d), 35k (e), and **aPEG2k-yTREN**, with **y** = 1.0, 1.2, 1.5 (f).

Table S2. Thermal data established by differential scanning calorimetry (T_m: melting temperature, χ_c: Degree of crystallization, ΔH_c: fusion enthalpy, ΔH_c for 100% crystalline **PEG** = 196.6 J g^{-1}).[27]

| Sample name	T_m (°C)	χ_c (%)	ΔH_c (J g^{-1})
PEG$_{1k}$	29	58%	114
aPEG$_{1k}$	22	53%	105
aPEG$_{1k}$-1.2TREN	-	-	-
PEG$_{2k}$	52	83%	163
aPEG$_{2k}$	41	70%	137
aPEG$_{2k}$-1.0TREN	39	41%	81
aPEG$_{2k}$-1.2TREN	38	38%	74
aPEG$_{2k}$-1.5TREN	35	34%	69
PEG$_{3k}$	61	84%	166
aPEG$_{3k}$	52	77%	151
aPEG$_{3k}$-1.2TREN	48	43%	85
PEG$_{10k}$	65	91%	178
aPEG$_{10k}$	60	77%	151
aPEG$_{10k}$-1.2TREN	57	61%	119
PEG$_{35k}$	66	80%	158
aPEG$_{35k}$	63	74%	146
aPEG$_{35k}$-1.2TREN	61	67%	131
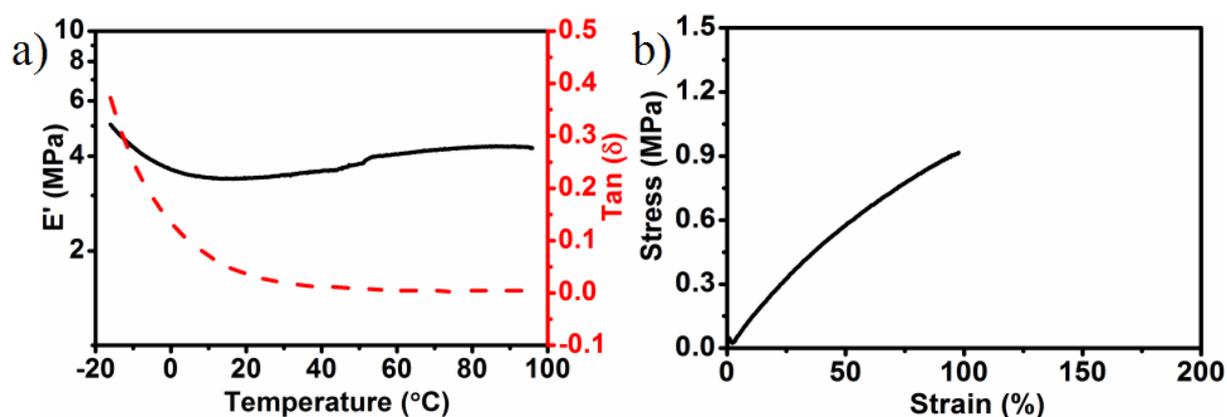
Figure S13. (a) DMA traces showing the storage modulus (*E'*, black solid line) and *tan(δ)* (red dashed line) as a function of temperature for **aPEG$_{1k}$-1.2TREN**. (b) Stress-strain curves of **aPEG$_{1k}$-1.2TREN**.
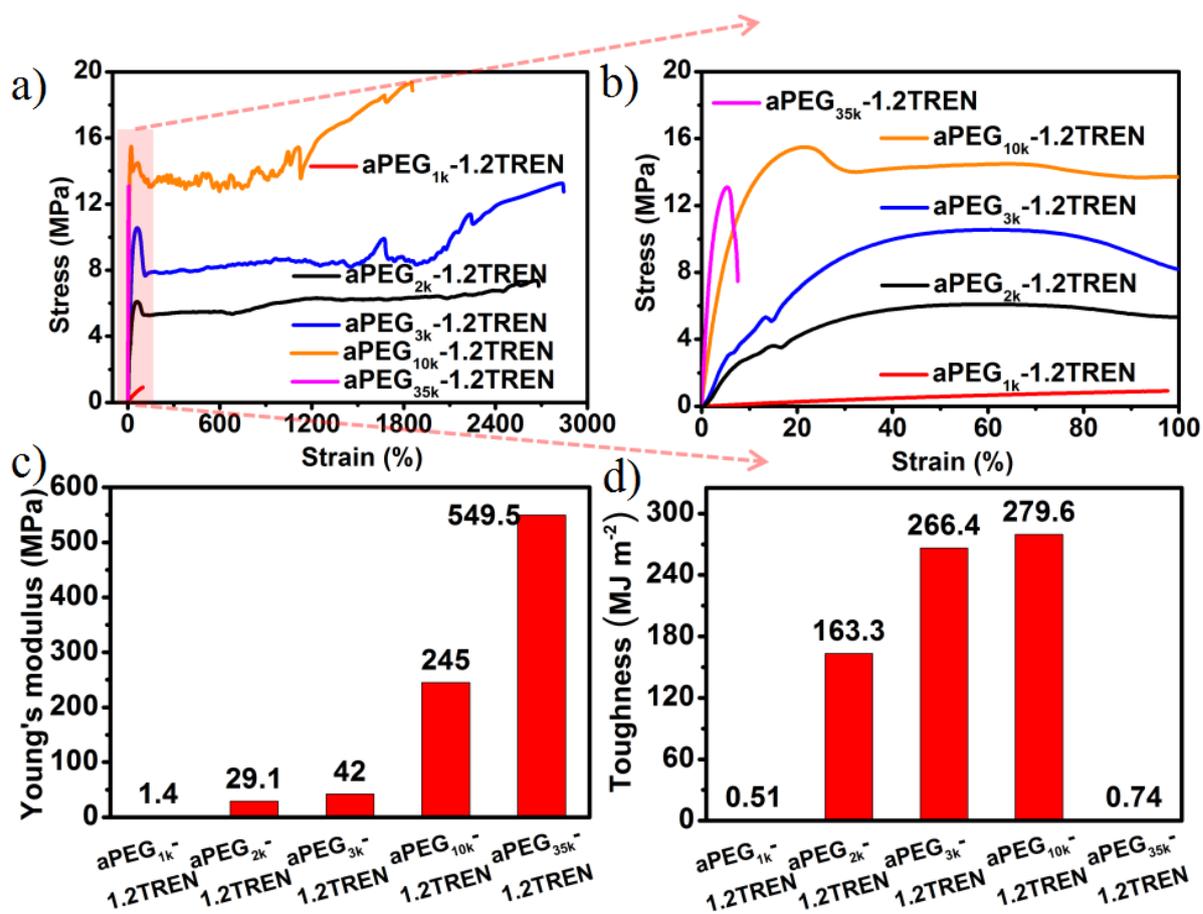
Figure S14. (a) Stress-strain curves, and (b) the expansion of the 0-100% strain regime, (c) Young's modulus, and (d) toughness for **aPEG$_x$-1.2TREN** with **x** = 1k (red), 2k (black), 3k (blue), 10k (orange), and 35k (magenta).

Table S3. Summary of the mechanical properties of **aPEG$_x$-1.2TREN** (length × width × thickness: $40 \times 5 \times 0.2$ mm).

| Sample name	Stress at break (MPa)	Strain at break (%)	Young's modulus (MPa)	Toughness (MJ m^{-3})
aPEG$_{1k}$-1.2TREN	0.8 ± 0.1	92 ± 15	1.3 ± 0.2	0.5 ± 0.1
aPEG$_{2k}$-1.2TREN	7.5 ± 0.6	2300 ± 419	28.5 ± 2.2	158.2 ± 8.4
aPEG$_{3k}$-1.2TREN	13.7 ± 0.7	3187 ± 461	44.5 ± 3.5	273.4 ± 11.5
aPEG$_{10k}$-1.2TREN	18.6 ± 0.9	1894 ± 195	246.3 ± 25.3	289.3 ± 12.4
aPEG$_{35k}$-1.2TREN	12.7 ± 0.8	8.7 ± 1	529.5 ± 38.2	0.7 ± 0.1
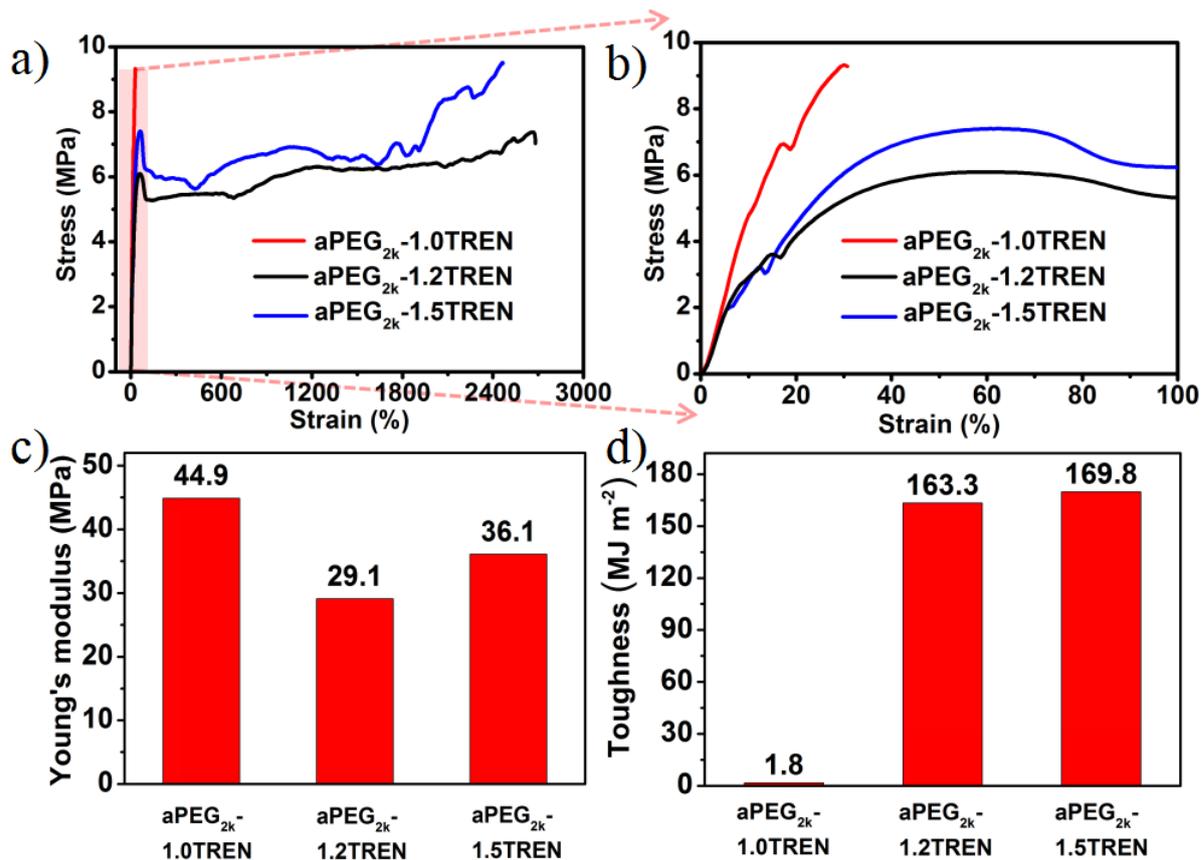
Figure S15. (a) Stress-strain curves, and (b) the expansion of the 0-100% strain regime, (c) Young's modulus, and (d) toughness for **aPEG$_{2k}$-yTREN**. **y** is 1.0 (red), 1.2 (black), 1.5 (blue).

Table S4. Summary of the mechanical properties of **aPEG$_{2k}$-yTREN** (length × width × thickness: 40 × 5 × 0.2 mm).

Sample name	Stress at break (MPa)	Strain at break (%)	Young's modulus (MPa)	Toughness (MJ m^{-3})
aPEG$_{2k}$-1.0TREN	9.3 ± 1.2	25 ± 7	44.5 ± 4.0	1.8 ± 0.8
aPEG$_{2k}$-1.2TREN	7.5 ± 0.6	2300 ± 419	28.5 ± 2.2	158.2 ± 8.4
aPEG$_{2k}$-1.5TREN	9.3 ± 0.4	2265 ± 232	35.1 ± 2.0	163.5 ± 9.1
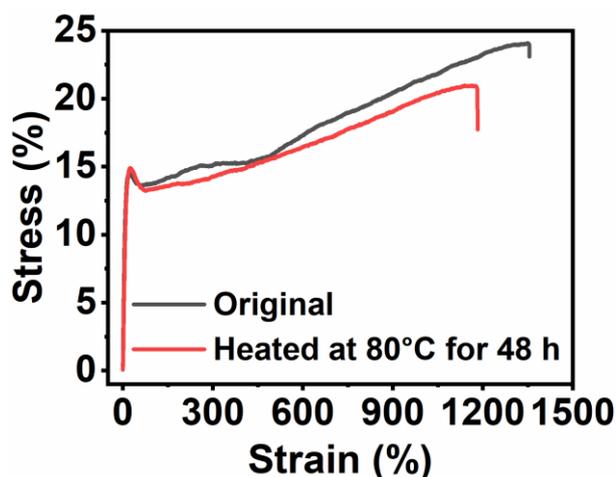
Figure S16. Stress-strain curves of **aPEG$_{10k}$-1.2TREN** before (black) and after (red) being heated in an oven at 80 °C for 48 h. The stress-strain measurements were conducted using a Zwick/Roell Z010 tensile tester equipped with a 500 N load cell and a strain rate of 100 mm·min^{-1}.
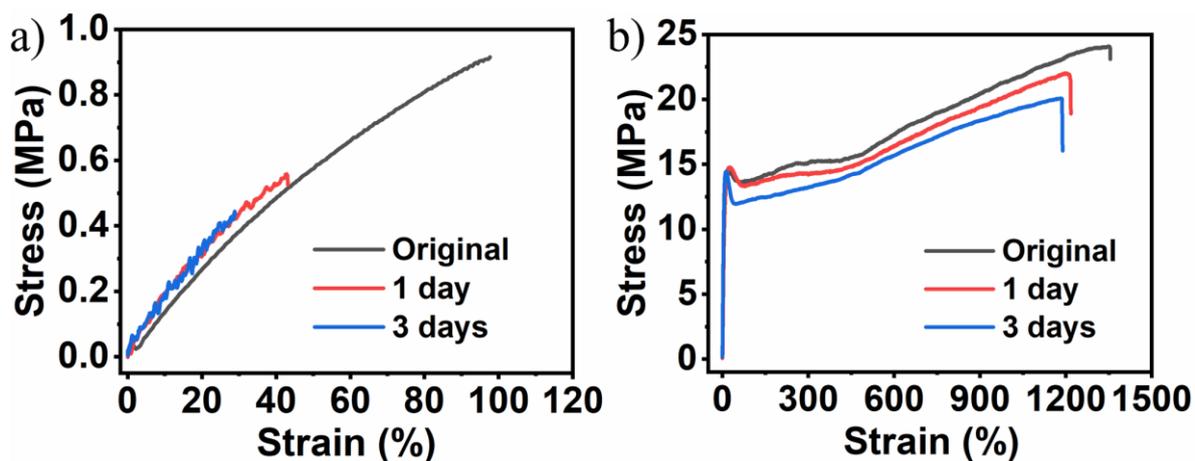
Figure S17. Stress-strain curves of **aPEG$_{1k}$-1.2TREN** (a) and **aPEG$_{10k}$-1.2TREN** (b) before (black) and after exposure to an 85% humidity environment for 1 day (red) or 3 days (blue). The 85% humidity environment was achieved by placing a 200 mL saturated KCl aqueous solution in an airtight desiccator with a diameter of 300 mm. The stress-strain measurements were conducted using a Zwick/Roell Z010 tensile tester equipped with a 500 N load cell and a strain rate of 100 mm·min^{-1}.
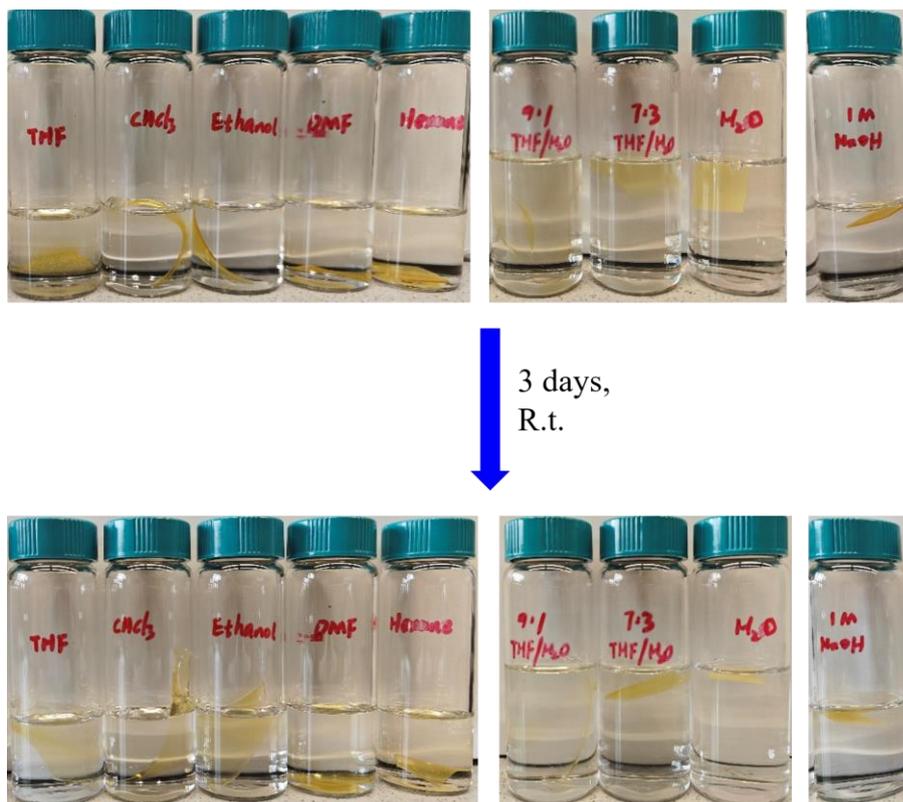
Figure S18. Photographs of **aPTHF₂ₖ-1.2TREN** dispersed in 5 mL of various organic solvents including THF, CHCl₃, ethanol, DMF, hexane (as indicated in the left column), and in 10 mL of water or THF/H₂O mixtures with volume ratios of 9:1 and 7:3, respectively (as indicated in the middle column), and in 5 mL of 1 M NaOH aqueous solution before (top row) and after (bottom row) a 3-day incubation period at room temperature.
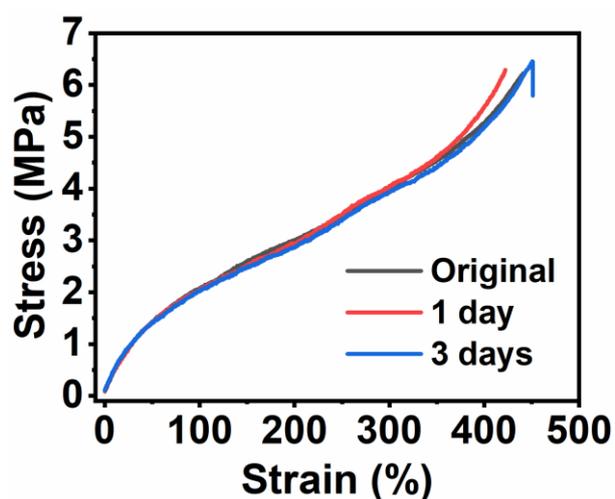
Figure S19. Stress-strain curves of **aPTHF₂ₖ-1.2TREN** before (black) and after exposure to 85% relative humidity for 1 day (red) or 3 days (blue). The 85% relative humidity environment was achieved by placing a 200 mL saturated KCl aqueous solution in an airtight desiccator with a diameter of 300 mm. The stress-strain measurements were conducted using a Zwick/Roell Z010 tensile tester equipped with a 500 N load cell and a strain rate of 100 mm·min⁻¹.

Synthesis of bis-(butyl vinylogous urethane)-terminated polyethylene glycol

In a 25 mL two-necked flask equipped with a reflux condenser and a magnetic stir bar, butylamine (**Btl**; 0.73 g, 10 mmol) was combined with **aPEG2k** (2.2 g, 1 mmol) in 10 mL of THF. The reaction mixture was heated to 60 °C for 24 h while stirring. The excess of **Btl** and THF was removed by rotary evaporation, followed by subsequent vacuum drying at 70 °C for 12 h. Bis-(butyl vinylogous urethane)-terminated polyethylene glycol (**aPEG2k-Btl**) was obtained as a brownish solid (2.3 g; yield 98 %).

^{1}H NMR (500 MHz, Chloroform-*d*) δ 8.53 (s, 1H), 4.48 (s, 1H), 4.19 (t, J = 5.0 Hz, 2H), 3.66 – 3.65 (m, 87H), 3.21 (q, J = 6.6 Hz, 2H), 2.09 (s, 3H), 1.55 (q, J = 7.3 Hz, 2H), 1.41 (q, J = 7.4 Hz, 2H), 0.95 (t, J = 7.3 Hz, 3H). The ^{1}H NMR spectrum is shown in Figure S20.
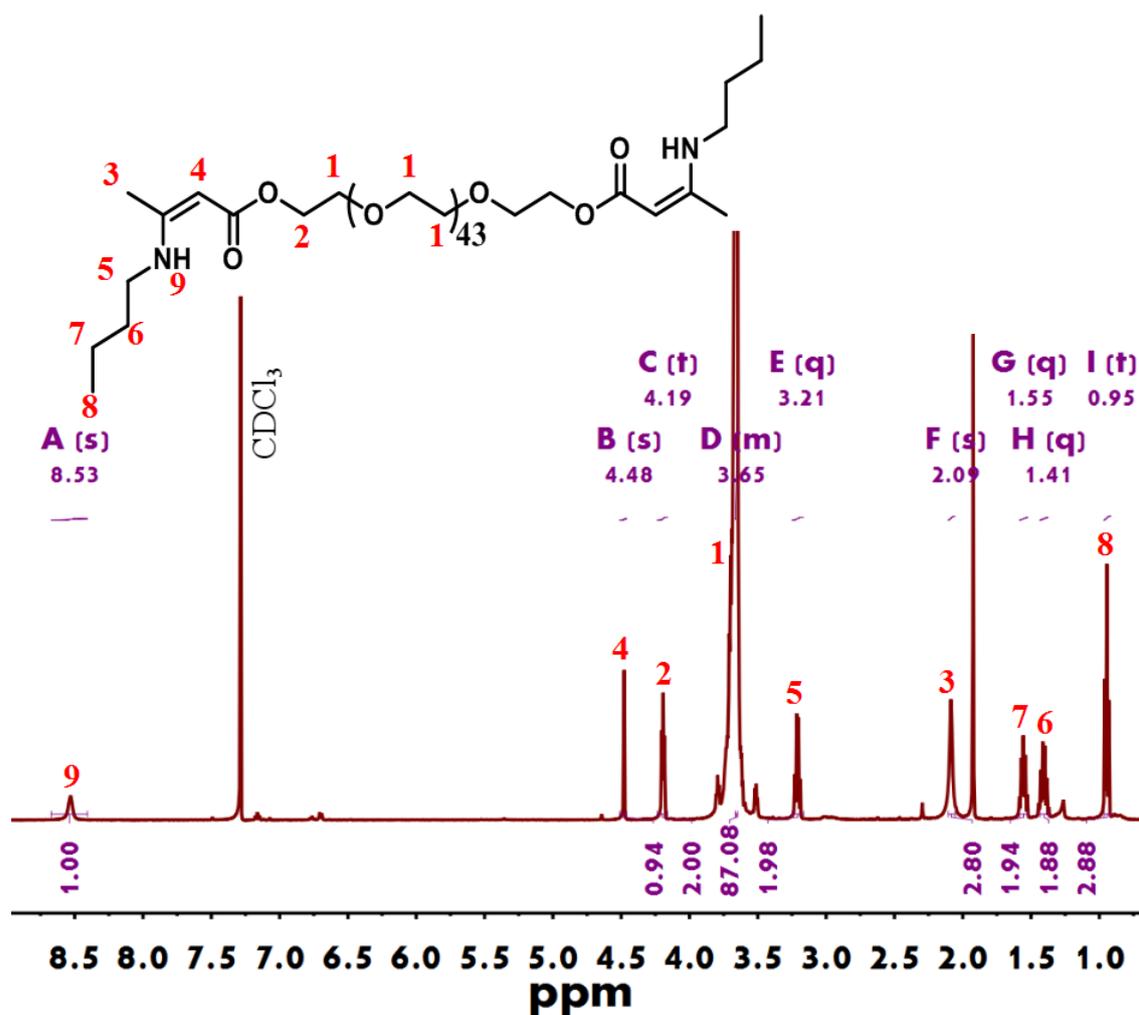

Figure S20. ^{1}H NMR spectrum (CDCl3, 500 MHz) of **aPEG2k-Btl**.

Kinetic measurements of the hydrolysis of aPEG$_{2k}$-Btl by *in situ* ^{1}H NMR spectroscopy

The influence of temperature on the hydrolysis of **aPEG$_{2k}$-Btl** was investigated according to the following procedures. 20 mg of **aPEG$_{2k}$-Btl** was added to 700 μL of **D$_2$O** solution in an NMR tube. The mixture was heated to different temperatures (25 °C, 40 °C, 60 °C) and the ^{1}H NMR spectra were measured at different time intervals (Figure S21), the proton assignment before and after the hydrolysis is shown in Figure S21(a).

The fraction of **aPEG$_{2k}$-Btl** was calculated by integration of the ^{1}H NMR signals (Figures S21b-d), according to the equation:

Fraction **aPEG$_{2k}$-Btl** = [**aPEG$_{2k}$-Btl**]/([**aPEG$_{2k}$-Btl**]+[**Btl**]) = Integral of proton 1/(Integral of proton 1 + Integral of proton 1').

The extent of conversion at specific temperatures is plotted in Figure S21(e).

The influence of water content on the hydrolysis of **aPEG$_{2k}$-Btl** was investigated according to the following procedures. 20 mg of **aPEG$_{2k}$-Btl** was added to different volumes of **D$_2$O** (200 μL, 300 μL, 500 μL, 700 μL) in an NMR tube. The mixture was kept at 25 °C and the ^{1}H NMR spectra were measured at different time intervals (Figure S22), the proton assignment before and after the hydrolysis is shown in Figure S22(a).

The fraction of **aPEG$_{2k}$-Btl** was calculated by integration of the ^{1}H NMR signals (Figures S22b-e), according to the equation:

Fraction **aPEG$_{2k}$-Btl** = [**aPEG$_{2k}$-Btl**]/([**aPEG$_{2k}$-Btl**]+[**Btl**]) = Integral of proton 1/(Integral of proton 1 + Integral of proton 1').

The extent of conversion with different volumes of **D$_2$O** present is plotted in Figure S22(f).
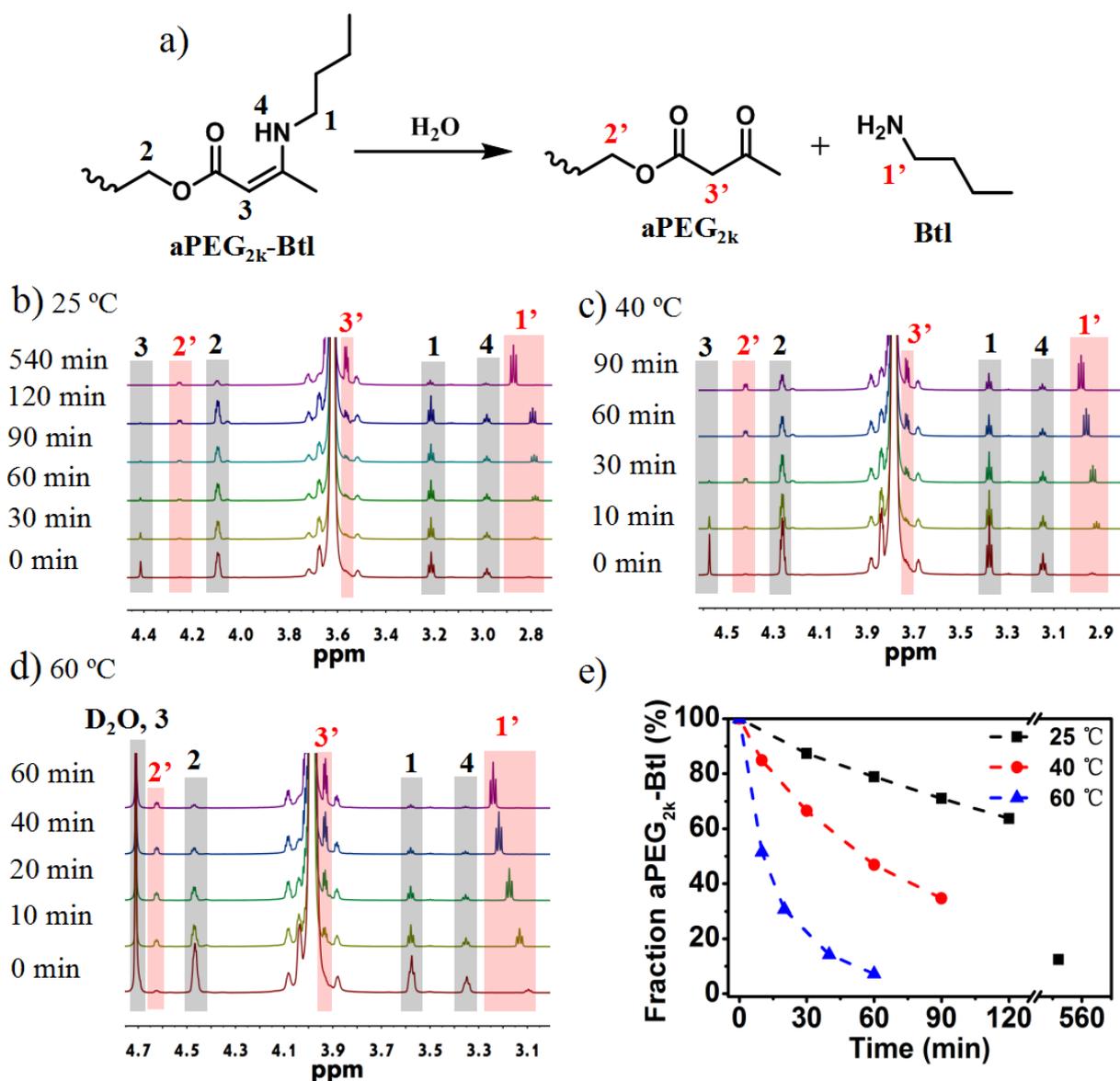
Figure S21. (a) Scheme showing the hydrolysis of **aPEG2k-Btl** into **aPEG2k** and **Btl**, with the assignment of the key protons for the integration of the ^{1}H NMR signals. Evolution of the ^{1}H NMR signals (D_2O, 700 MHz) of the reaction mixtures containing **aPEG2k-Btl** (20 mg) and D_2O (700 μL). The samples were collected at different reaction times (as indicated), and the reactions were carried out at (b) 25 °C, (c) 40 °C, and (d) 60 °C. (e) Extent of conversion of **aPEG2k-Btl** into **aPEG2k** and **Btl** measured as a function of time at 25 ℃ (black), 40 ℃ (red), and 60 ℃ (blue) with 0.7 mL of D_2O present. The molar fraction of **aPEG2k-Btl** (Fraction **aPEG2k-Btl** (%)) was determined by integration of the ^{1}H NMR signals shown in (b)-(d). The dashed lines are a simple guide to the eye.
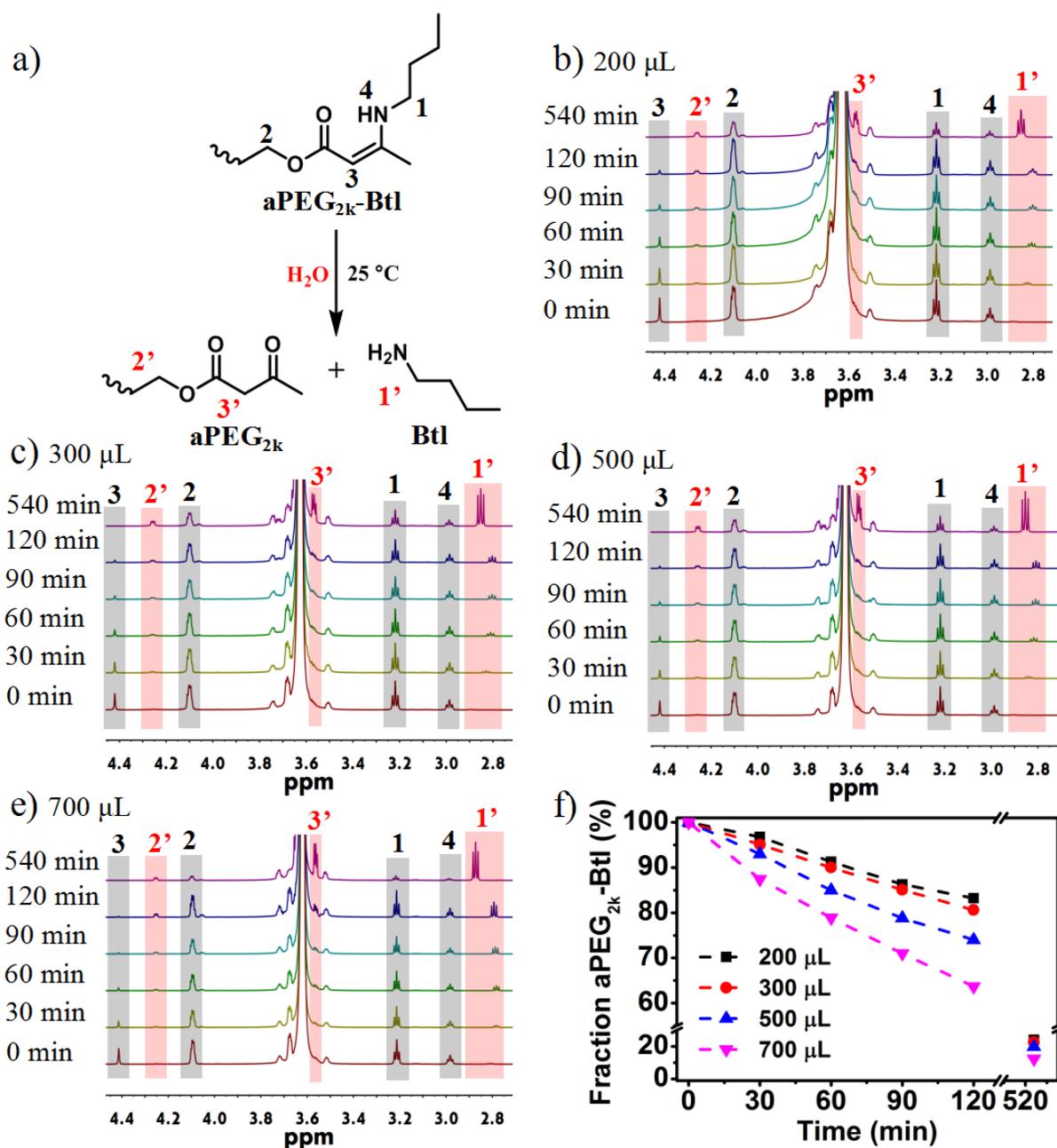
Figure S22. (a) Scheme showing the hydrolysis of **aPEG$_{2k}$-Btl** into **aPEG$_{2k}$** and **Btl**, with the assignment of the key protons for the integration of the ^{1}H NMR signals. Evolution of the ^{1}H NMR signals (D$_2$O, 700 MHz) of the reaction mixtures containing **aPEG$_{2k}$-Btl** (20 mg) and different volumes of **D$_2$O** (200, 300, 500, 700 μL) at 25 °C. The samples were collected at different reaction times (as indicated), and the reactions were carried out in (b) 200 μL, (c) 300 μL, (d) 300 μL, and (e) 700 μL of **D$_2$O**. (f) Extent of conversion of **aPEG$_{2k}$-Btl** into **aPEG$_{2k}$** and **Btl** measured as a function of time with 200 μL (black), 300 μL (red), 500 μL (blue) and 700 μL (magenta) of **D$_2$O** present. The molar fraction of **aPEG$_{2k}$-Btl** (Fraction **aPEG$_{2k}$-Btl** (%)) was determined by integration of the ^{1}H NMR signals shown in (b)-(e). The dashed lines are a simple guide to the eye.

Determination of the activation energies for the hydrolysis of aPEG$_{2k}$-Btl with D$_2$O

The rate constants (k) for the hydrolysis of **aPEG$_{2k}$-Btl** with **D$_2$O** were obtained by monitoring the fraction of **aPEG$_{2k}$-Btl** in the reaction mixtures (Figures S21b-d) under pseudo-first-order conditions (large excess of **D$_2$O**) (Supplementary Equation 1). The activation energies ΔE for the small molecule reactions were determined by plotting $\ln(k)$ vs. T^{-1} (Supplementary Equation 2).

Supplementary Equations (1):

$\ln(\text{fraction } \textbf{aPEG}_{2k}\textbf{-Btl}) = -k(\text{t})$, the fitting curves are shown in Figure S23.

Supplementary Equation (2):

$\ln(k) = \ln(A) - \Delta E/RT$, the fitting curve is shown in Figure 3c.

where T is the temperature expressed in Kelvin, and R = 8.31 J K^{-1} mol^{-1}. The values for k and ΔE thus determined are shown in Table S5.
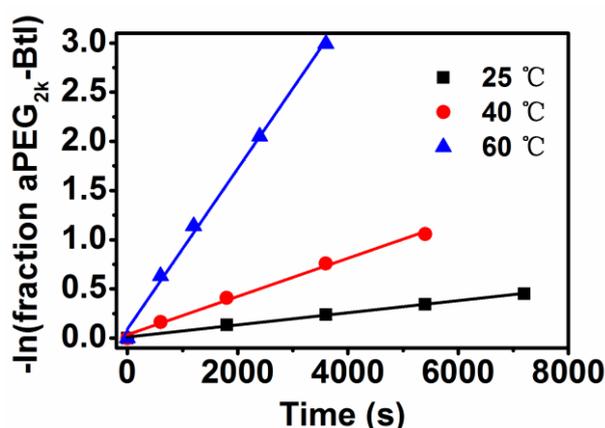
Figure S23. Fitting curves for the hydrolysis between **aPEG$_{2k}$-Btl** and an excess of **D$_2$O** at 25 ℃ (black), 40 ℃ (red), and 60 ℃ (blue).

Table S5. Pseudo-first-order rate constants (k) and activation energy (E_a) for the hydrolysis between **aPEG$_{2k}$-Btl** and an excess of **D$_2$O**.

Temperature (°C)	Rate constants k (s^{-1})	Activation energy E_a (kJ mol^{-1})
25	6.17E-05	
40	1.94E-04	61
60	8.15E-04	

Hydrolysis of aPEG$_{2k}$-1.2TREN monitored by pH variations

Since the hydrolysis of vinylogous urethane releases alkaline amines, the process could be monitored by measuring the pH of the H$_2$O phase. As shown in Figure S24(a), 0.2 g of **aPEG$_{2k}$-1.2TREN** debris was treated with 2 mL of H$_2$O. The pH of the H$_2$O phase was measured with a pH meter (SevenExcellence S400-Micro, Mettler Toledo, Switzerland) at specific times. The evolution of pH measured as a function of time is shown in Figure S24(b).
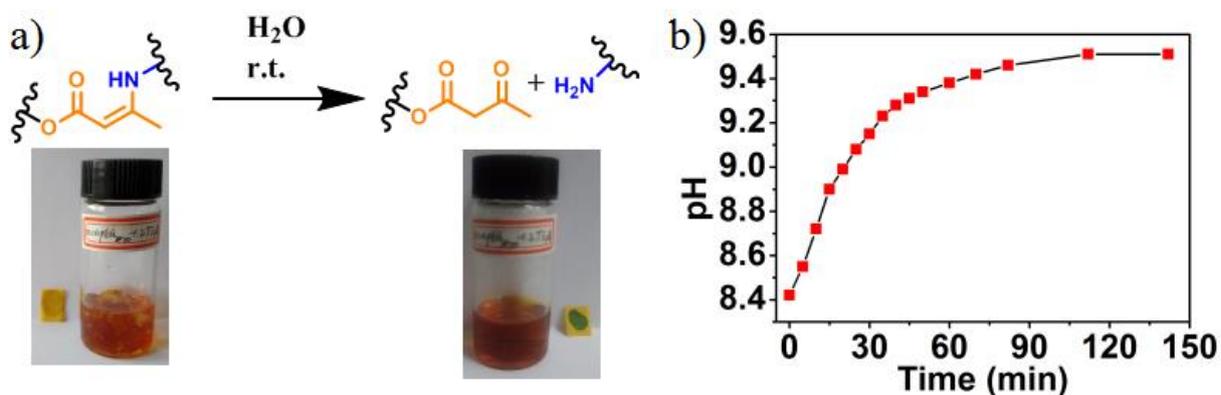
Figure S24. (a) Hydrolysis of vinylogous urethane, and pictures showing the dissolution of the components of **aPEG$_{2k}$-1.2TREN** over time, after being treated with 2 mL of H$_2$O. The dissolution is accompanied by an increase of the pH of the water phase, as suggested by the change in color of the indicator from yellow (left) to green (right) after the deposition of a drop of the water phase into pH paper. (b) Variation of the pH value of the water phase of the reaction shown in (a), showing an initial pH of 8.4, and a pH of ca. 9.6 after 150 min.

Depolymerization of aPEG$_{2k}$-1.2TREN observed by *in situ* ^{1}H NMR spectroscopy

20 mg of **aPEG$_{2k}$-1.2TREN** was added to 0.55 mL of D$_2$O solution in an NMR tube. The mixture was heated to different temperatures (20 °C, 40 °C, 60 °C, 80 °C) and the ^{1}H NMR spectra were measured at different time intervals (Figures S25b-e). Peak ***m*** (red areas) refers to the characteristic protons of the ethylene segments in **aPEG$_{2k}$-1.2TREN** (Figure S25a). Peak ***n*** (orange areas) is assigned to D$_2$O. Assuming that the evaporation of D$_2$O is negligible, relative depolymerization degree (**RDD**) could be calculated by integration of the ^{1}H NMR spectra (Figures S25b-e), according to the equation:

RDD (%) = (***m$_t$*** - ***m$_0$***)/***m***$_0$,

where ***m$_t$*** is the ratio of peak ***m*** at t time to peak ***n*** at t time and ***m$_0$*** is the ratio of peak ***m*** at initial time to peak ***n*** at initial time.

The calculated relative depolymerization degrees are plotted in Figure S25(f).
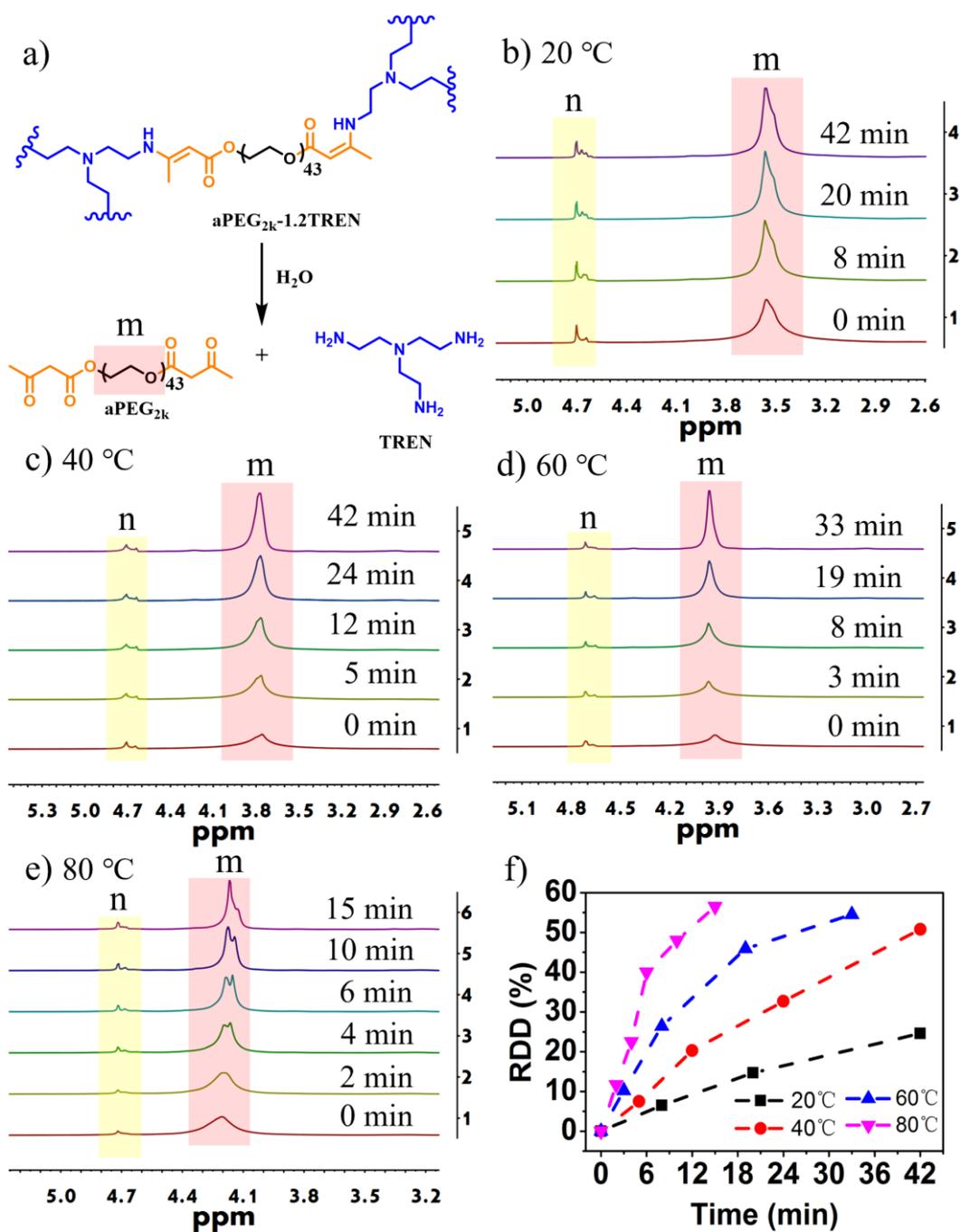
Figure S25. (a) Scheme showing the hydrolysis of **aPEG₂ₖ-1.2TREN** into **aPEG₂ₖ** and **TREN**. The red area highlights the characteristic protons of the ethylene segment (peak *m*). Evolution of the ¹H NMR signals (D₂O, 500 MHz) of the reaction mixtures containing **aPEG₂ₖ-1.2TREN** (20 mg) and **D₂O** (0.55 mL). The samples were collected at different reaction times (as indicated), and the reactions were carried out at (b) 20 °C, (c) 40 °C, (d) 60 °C, (e) 80 °C. Peak *n* is assigned to D₂O. (f) Relative depolymerization degree (**RDD**) of **aPEG₂ₖ-1.2TREN** into **aPEG₂ₖ** and **TREN** measured as a function of time at 20 ℃ (black), 40 ℃ (red), and 60 ℃ (blue) and 80 ℃ (magenta) with 0.55 mL of **D₂O** present. The dashed lines are a simple guide to the eye. **RDD** (%) = (m_t - m_0)/m_0.

Determination of the dissolution time for aPEG$_x$-1.2TREN

0.2 g of **aPEG$_x$-1.2TREN** debris (**x** = 1k, 2k, 3k, 10k, 35k) was added to 3 mL of deionized H$_2$O solution in a vial. The cross-linked film dissolved over time, which resulted in a clear solution (Figure S28, first two lines). The dissolution time is defined by measuring the total time for the gel-to-sol transition of each polymer. The gel-to-sol transition was determined by whether the solution could successfully pass through a 0.33 mm-diameter needle of 1 mL syringe. The thus determined dissolution time is shown in Figure S29.

Recovery of aPEG$_x$

The solutions obtained from the procedure discussed above were used to recover **aPEG$_x$**. First, 0.2 g of strongly acidic ion exchange resin (DOWEX 50WX8-10, Sigma-Aldrich) was added to the depolymerized solutions. The resulting mixture was shaken for 10 min. The ion exchange resins were filtered off by vacuum filtration. The obtained solutions were washed by activated charcoal three times in which the activated charcoal was filtrated out after each washing treatment. The solvent (H$_2$O) was removed by rotary evaporation, and the obtained material (**aPEG$_x$**) was further dried by vacuum oven at 80 °C for 24 h.

Recovered **aPEG$_{1k}$**: 98.8 %, 180.0 mg. ^{1}H NMR (400 MHz, Chloroform-d) δ 4.30 (ddd, J = 4.8, 4.0, 1.4 Hz, 2H), 3.73 – 3.71 (m, 2H), 3.64 (d, J = 1.4 Hz, 41H), 3.49 (d, J = 1.2 Hz, 2H), 2.28 (d, J = 1.2 Hz, 3H).

Recovered **aPEG$_{2k}$**: 97.5 %, 180.5 mg. ^{1}H NMR (400 MHz, Chloroform-d) δ 4.35 – 4.28 (m, 2H), 3.73 (dd, J = 3.3, 1.5 Hz, 2H), 3.66 (s, 89H), 3.50 (s, 2H), 2.29 (s, 3H).

Recovered **aPEG$_{3k}$**: 97.9 %, 188.9 mg. ^{1}H NMR (400 MHz, Chloroform-d) δ 4.34 – 4.29 (m, 2H), 3.74 – 3.73 (m, 2H), 3.66 (s, 133H), 3.50 (d, J = 3.4 Hz, 2H), 2.29 (s, 3H).

Recovered **aPEG$_{10k}$**: 98.6 %, 194.9 mg. ^{1}H NMR (400 MHz, Chloroform-d) δ 4.35 – 4.29 (m, 2H), 3.74 – 3.73 (m, 2H), 3.66 (s, 455H), 3.50 (d, J = 3.3 Hz, 2H), 2.29 (s, 3H).

Recovered **aPEG$_{35k}$**: 98.2 %, 196.4 mg. ^{1}H NMR (500 MHz, Chloroform-d) δ 4.32 (s, 2H), 3.73 (s, 2H), 3.66 (s, 1581H), 3.52 (s, 2H), 2.29 (s, 3H).

The comparisons between the ^{1}H NMR spectra of the original and recovered **aPEG$_x$** are shown in Figures S30-34.

Recovery of aPTHF$_{2k}$

0.2 g of little pieces of **aPTHF$_{2k}$-1.2TREN** was added to 5 mL of 1 M HCl aqueous solution in a vial (Figure S26a, left) and the mixture was stirred at 500 rpm min^{-1} using a stirring bar. After three days, the cross-linked film underwent degradation, leading to the formation of an off-white slurry that adhered to both the vial wall and the stir bar (Figure S26a, middle). The slurry was then extracted from the mixture by adding 5 mL of CHCl$_3$, and the collected CHCl$_3$ phase was washed three times with deionized water (Figure S26a, right). Finally, the CHCl$_3$ solvent was removed via rotary evaporation, followed by vacuum drying at 80 °C for 24 h. This process yielded a pale yellow liquid (**aPTHF$_{2k}$**).

Recovered **aPTHF$_{2k}$**: 95.0%, 179 mg. ^{1}H NMR (400 MHz, CDCl$_3$) δ 4.10 (t, J = 6.5 Hz, 2H), 3.38 (s, 2H), 3.36 – 3.32 (m, 61H), 2.20 (s, 3H), 1.55 (p, J = 3.0 Hz, 60H).

The comparison between the ^{1}H NMR spectra of the original and recovered **aPTHF$_{2k}$** is shown in Figure S26(b).
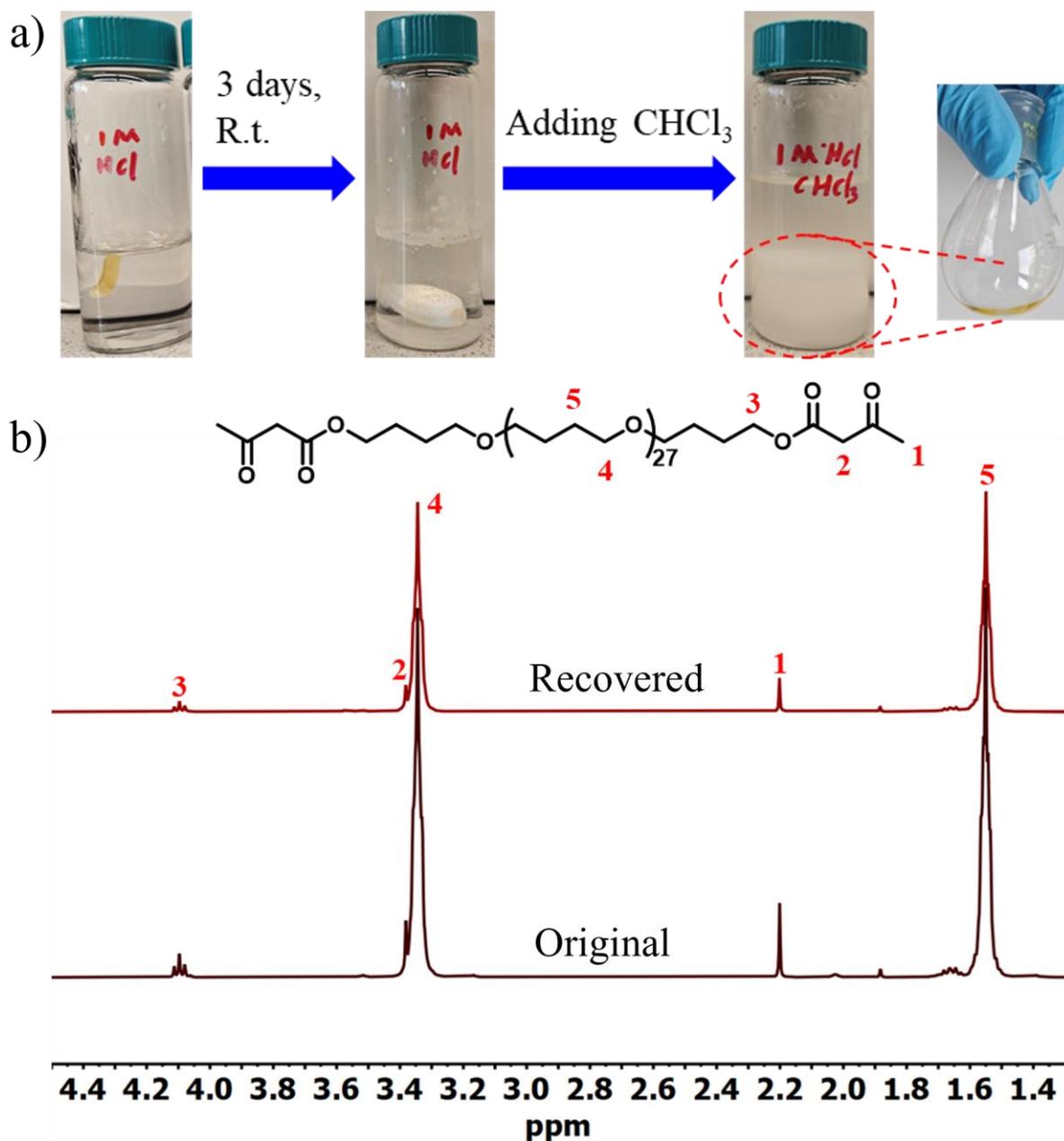
Figure S26. (a) Photographs showing the depolymerization of **aPTHF₂ₖ-1.2TREN**. The left picture shows the initial state of 0.2 g **aPTHF₂ₖ-1.2TREN** in 5 mL deionized water. After 3 days of depolymerization at room temperature, the polymer degraded and afforded an off-white slurry (middle). The **aPTHF₂ₖ** obtained from the depolymerization process could be recovered by an extraction process using CHCl₃, followed by vacuum drying (right). (b) Comparison between the ^{1}H NMR spectra of the initial and recovered **aPTHF₂ₖ**.

Model experiment for the recovery of TREN

The ion exchange resins filtered off during the procedure described above could, in principle, be used to recover **TREN**. However, the low amount of **TREN** used in **aPEG$_x$-yTREN** ($<$ 150 mg) made its recovery challenging, which ultimately resulted in the difficulty to estimate the recovery of this component. Thus, relying on a strategy developed by the Helms group,[10] we conducted a model experiment to demonstrate the possibility to recover **TREN**. First, 2 g of strongly acidic ion exchange resins were added to **TREN** (0.5 g) in deionized H$_2$O (10 mL) to absorb **TREN** (Figure S27i). The **TREN**-enriched ion exchange resins were filtered off by vacuum filtration. Then, 5 mL of **TEA** was mixed with the resins, and the mixture was shaken for 30 min. The suspension was filtered to recover the ion exchange resins for re-use. After evaporation of the volatiles (H$_2$O and excess **TEA**) by rotary evaporation, the recovered **TREN** was dried in vacuum oven at 70 °C (Figure S27).

Recovered **TREN**: 0.43 g, 86%. ^{1}H NMR (400 MHz, CDCl$_3$) δ 2.68 (p, J = 5.9 Hz, 1H), 2.44 (qd, J = 6.0, 2.5 Hz, 1H), 1.32 (s, 1H).

The comparison between the ^{1}H NMR spectra of the original and recovered **TREN** is shown in Figure S35.
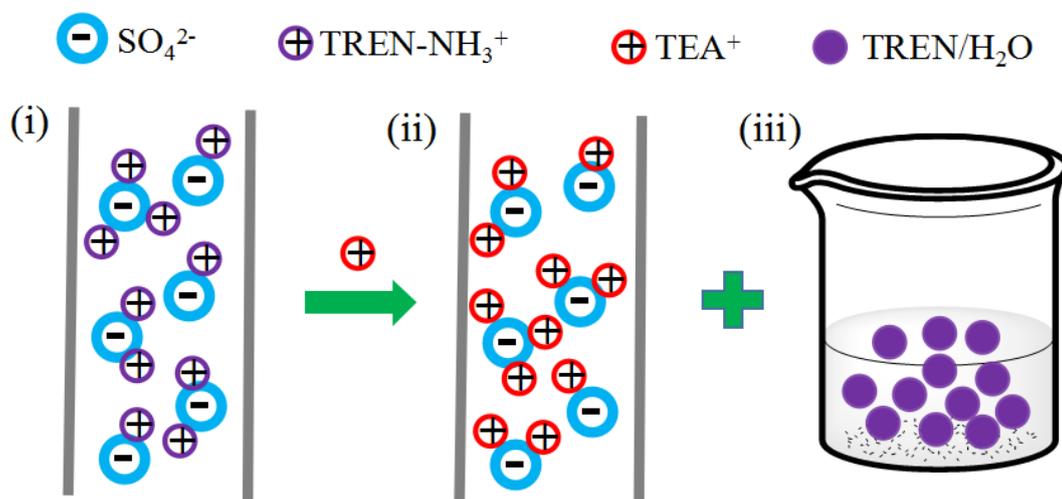
Figure S27. Recovery of **TREN** from the strongly acidic ion exchange resins.
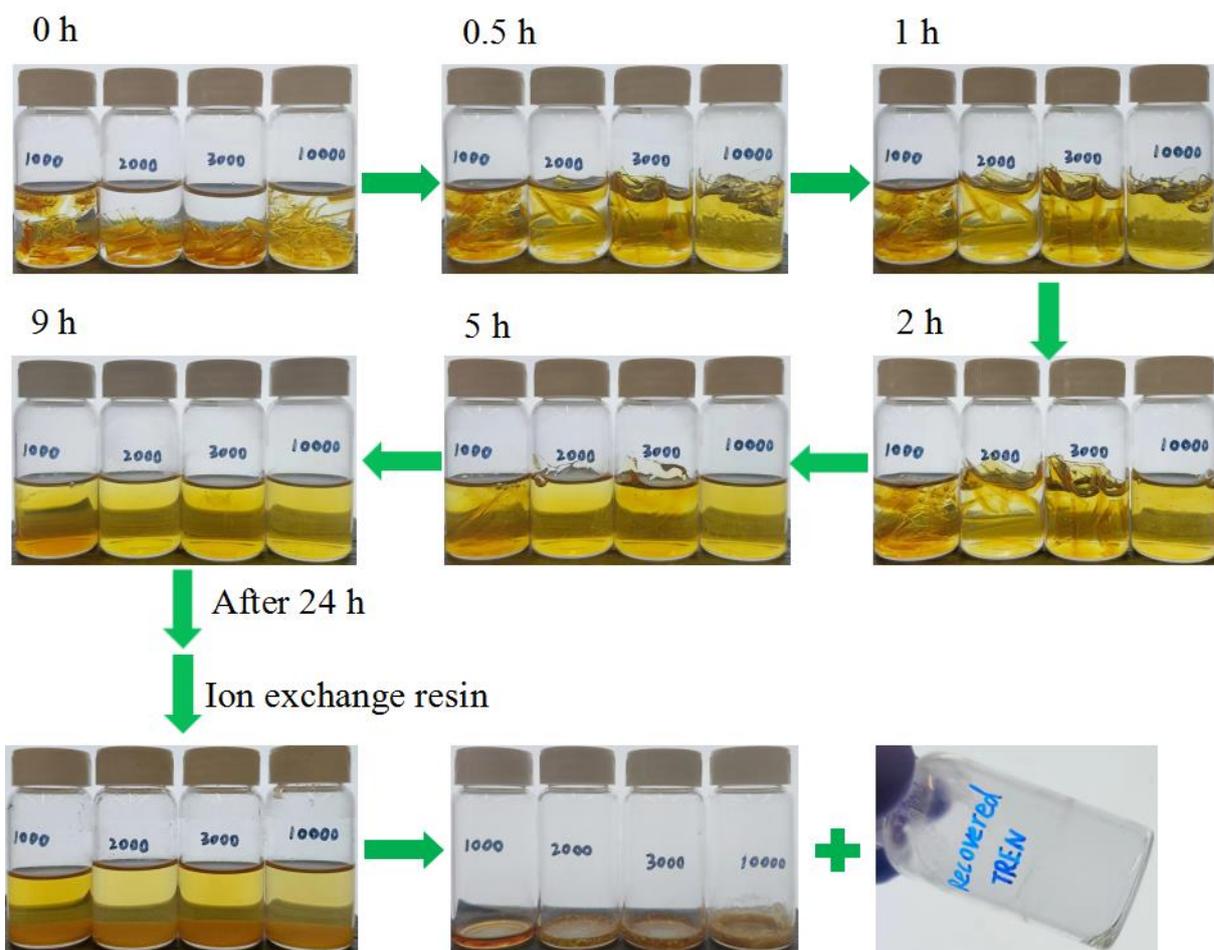
Figure S28. Photographs showing the depolymerization of **aPEGx-1.2TREN** by deionized water as a function of time (first two lines), followed by the separation and recovery of **aPEGx** and **TREN** (last line). The number on each vial indicates **x**, i.e., the molecular weight of each **aPEGx** used.
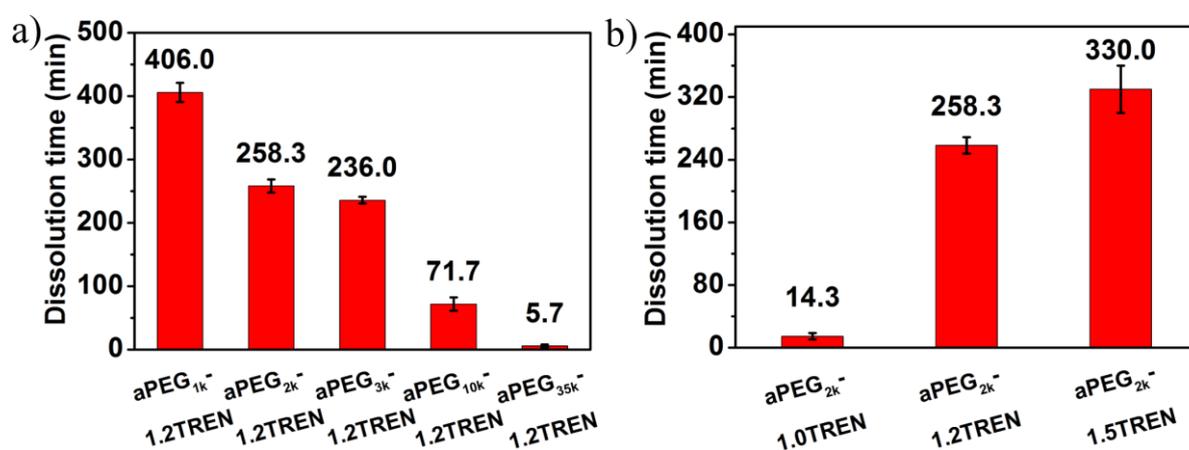

Figure S29. Dissolution time of **aPEGx-1.2TREN** (a) and **aPEG2k-yTREN** (b). The dissolution time is defined by measuring the time in which the gel-to-sol transition occurred (for the definition see page S27).

Figure S30. Comparison between the ^{1}H NMR spectra (CDCl$_3$, 400 MHz) of the original and recovered **aPEG$_{1k}$**.
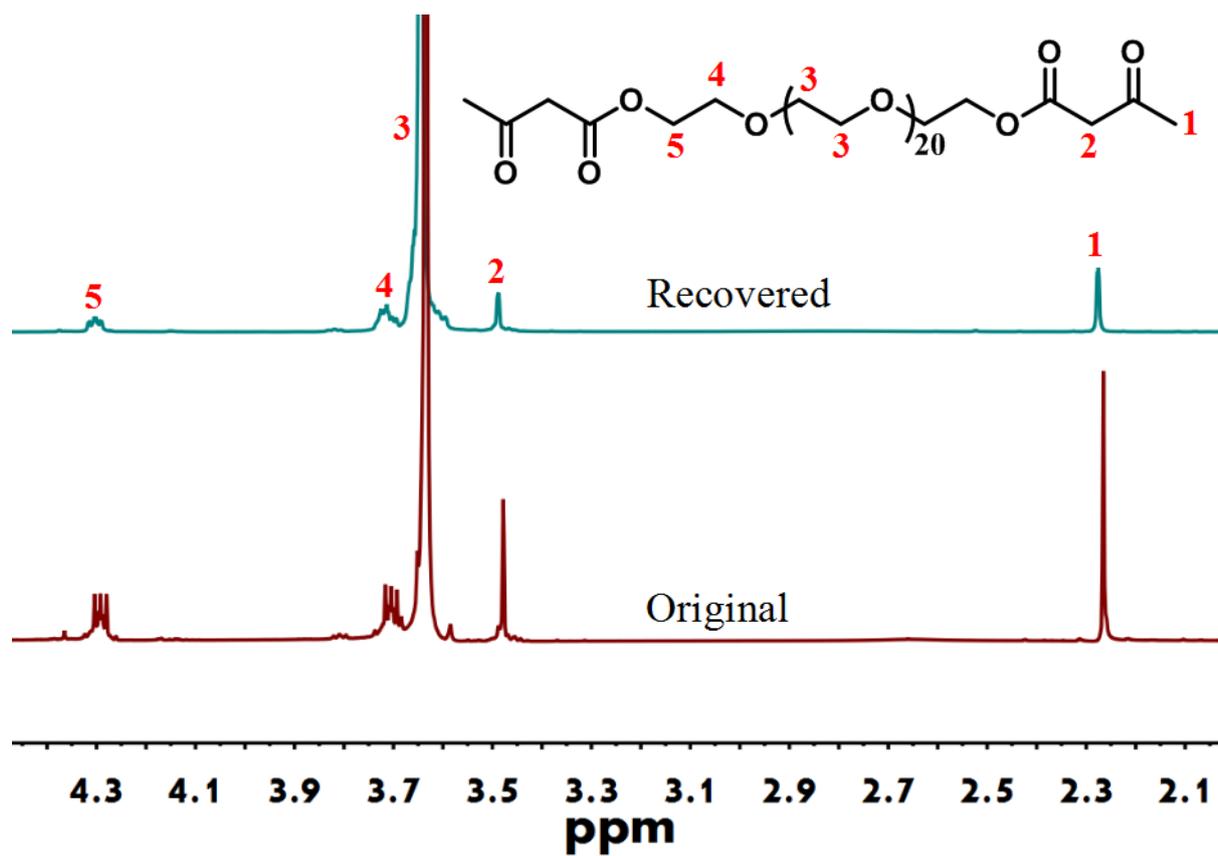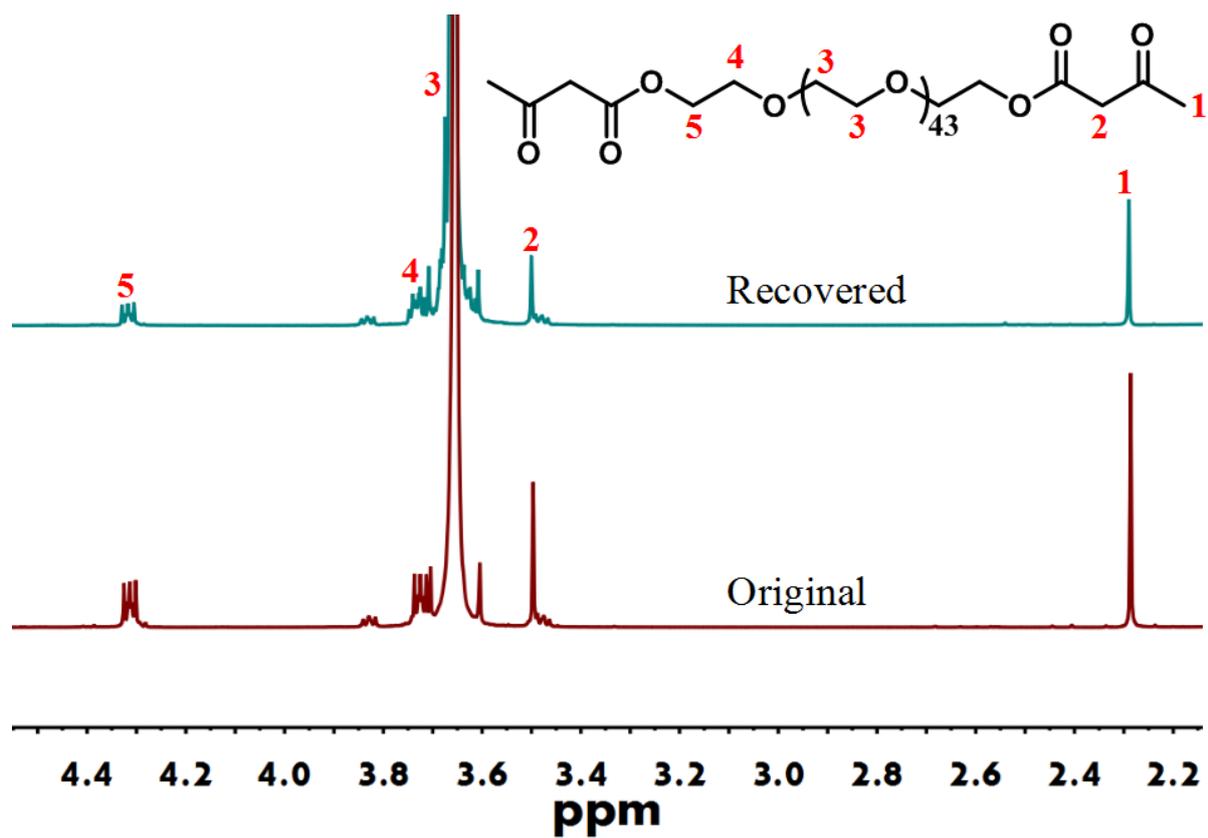
Figure S31. Comparison between the ^{1}H NMR spectra (CDCl$_3$, 400 MHz) of the original and recovered **aPEG$_{2k}$**.
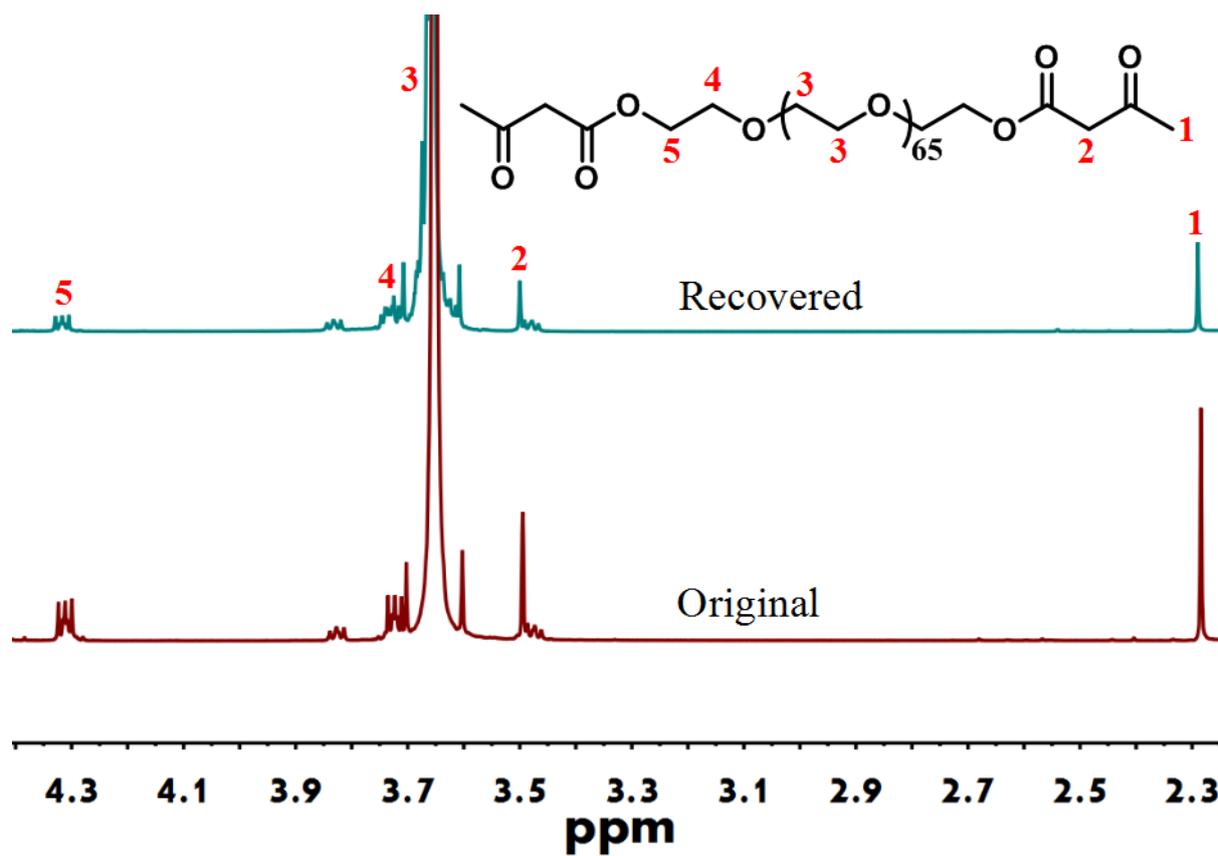
Figure S32. Comparison between the ^{1}H NMR spectra (CDCl$_3$, 400 MHz) of the original and recovered **aPEG$_{3k}$**.
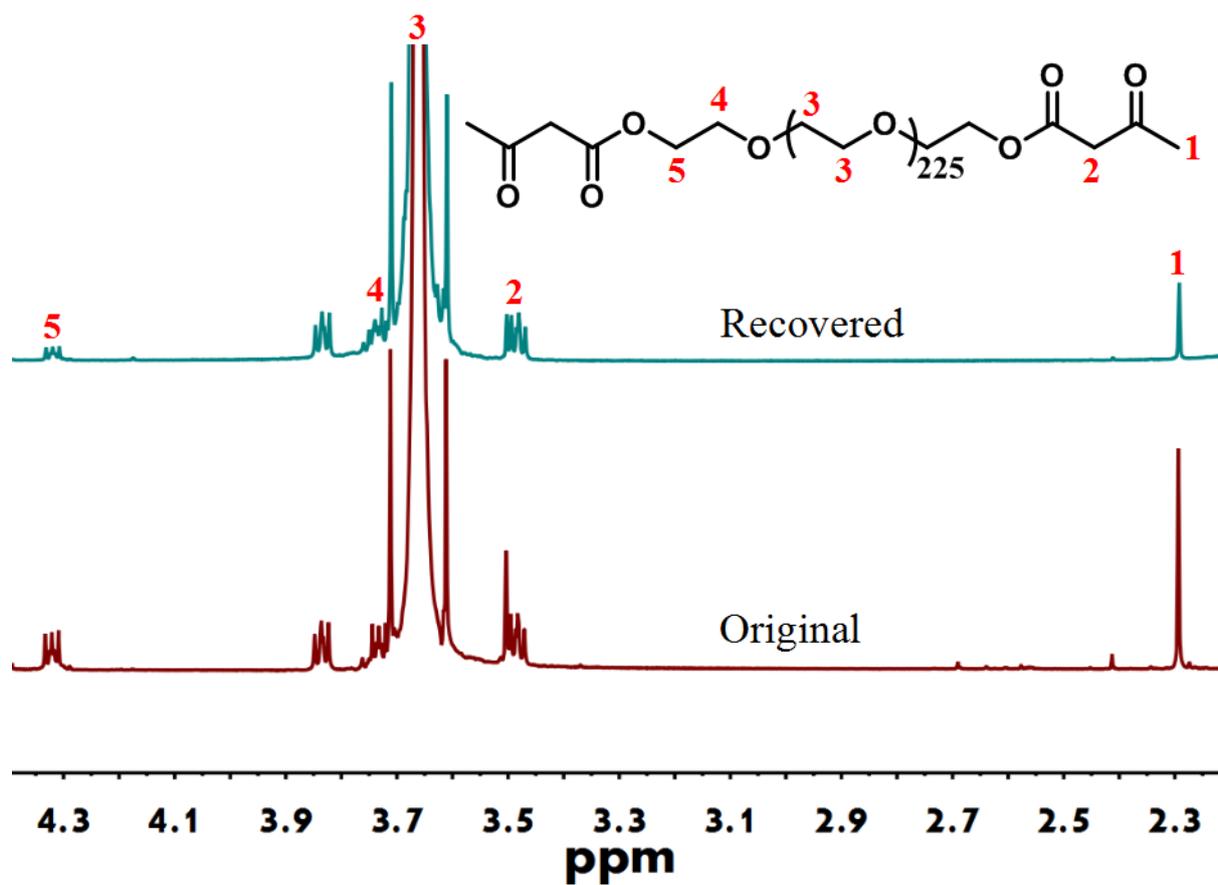
Figure S33. Comparison between the ^{1}H NMR spectra (CDCl$_3$, 400 MHz) of the original and recovered **aPEG$_{10k}$**.
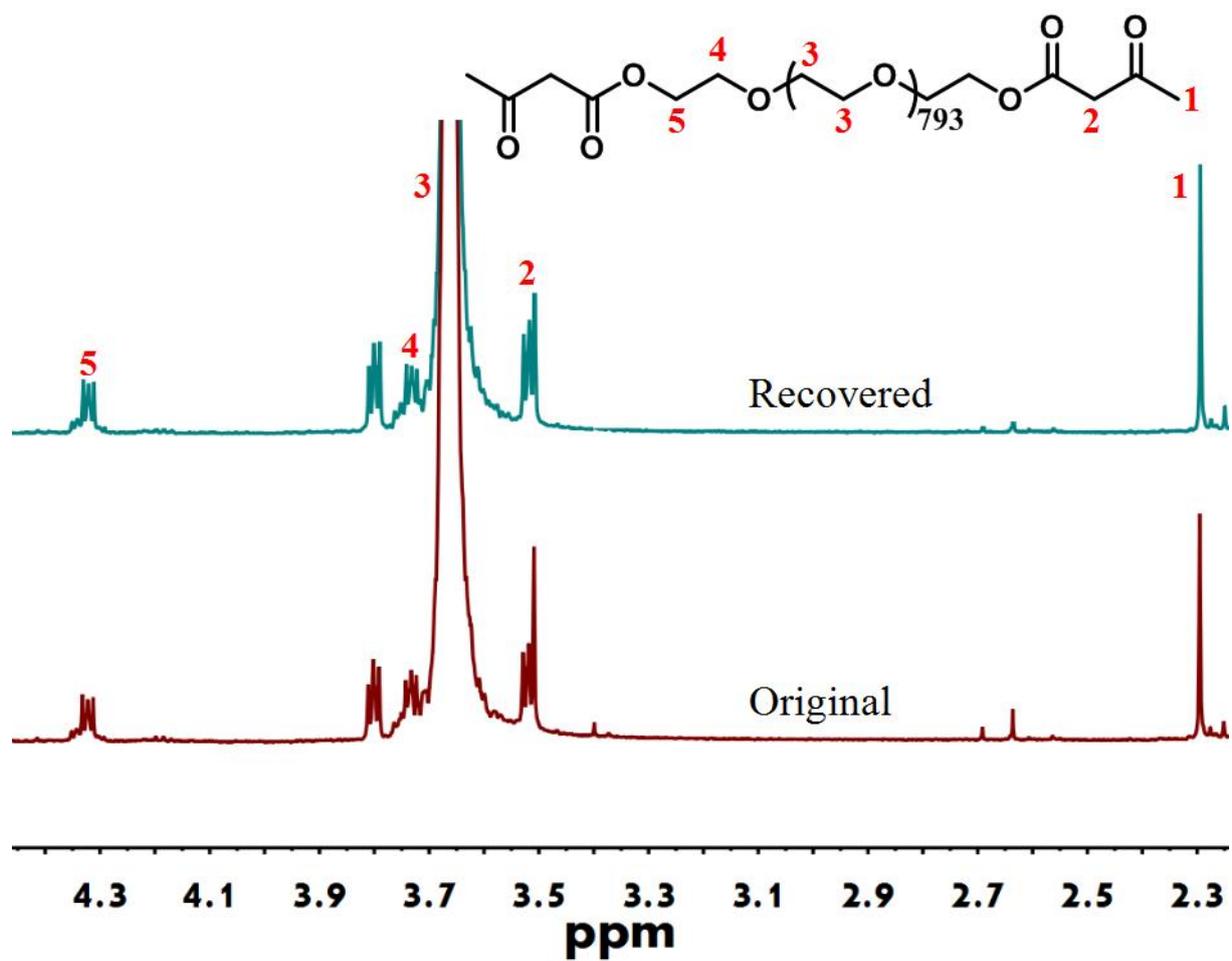
Figure S34. Comparison between the ^{1}H NMR spectra (CDCl$_3$, 400 MHz) of the original and recovered **aPEG$_{35k}$**.
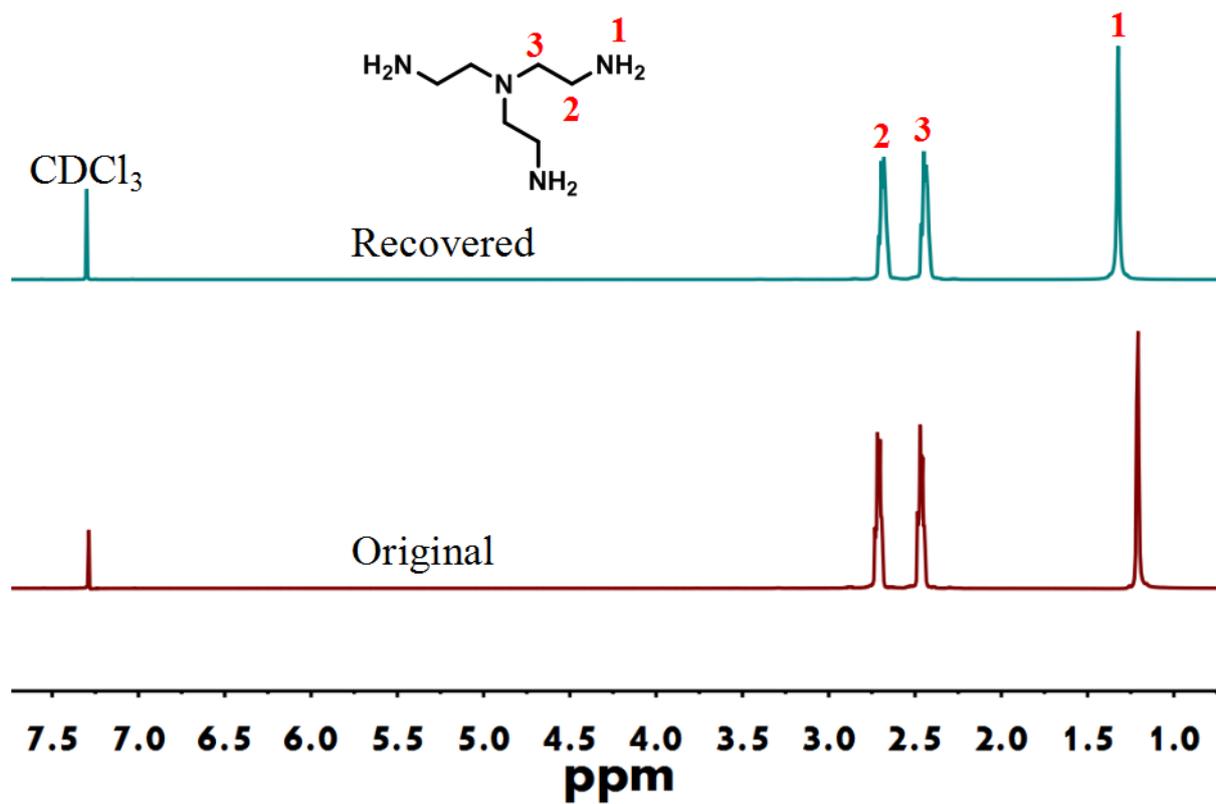
Figure S35. Comparison between the ^{1}H NMR spectra (CDCl$_3$, 400 MHz) of the original and recovered **TREN**.

Synthesis of aPEG$_{10k}$-1.2TREN/MCNs

aPEG$_{10k}$ (1.02 g, 0.1 mmol) and multi-walled carbon nanotubes (**MCNs**, 50 mg) were mixed in 5 mL of DMF in a 10 mL vial. Subsequently, **TREN** (11.6 mg, 0.08 mmol) was added to the mixture, which was stirred for 10 min. The resulting solution was poured onto a Teflon mold. The mixture was heated to 80 °C in a drying oven for 12 h, and then it was dried by vacuum oven at 80 °C for another 24 h. Vitrimer composite **aPEG$_{10k}$-1.2TREN/MCNs** was obtained as a black solid.

Depolymerization and recovery of starting materials from aPEG$_{10k}$-1.2TREN/MCNs

aPEG$_{10k}$-1.2TREN/MCNs (0.2 g) was treated with deionized H$_2$O (4 mL). The mixture was kept at room temperature for 24 h (Figure S36). After this time, **aPEG$_{10k}$-1.2TREN** was completely dissolved, and **MCNs** could be recovered by vacuum filtration. The morphology and chemical structure of the recovered **MCNs** were investigated by SEM technique equpped with Raman analysis and then compared with that of the original **MCNs** (Figure S37). The filtered solution was first treated with 0.2 g of strongly acidic ion exchange resins. The resin was filtered off, and the liquid phase was concentrated by rotary evaporation. After drying in a vacuum oven at 70 °C for 24 h, **aPEG$_{10k}$** was recovered (Figure S36, red dashed box).

Recovered **aPEG$_{10k}$**: 96.2 %, 181.4 mg. ^{1}H NMR (400 MHz, Chloroform-d) δ 4.34 – 4.28 (m, 2H), 3.75 (s, 2H), 3.65 (s, 492H), 3.50 (s, 2H), 2.29 (d, J = 0.7 Hz, 3H).

The comparison between the ^{1}H NMR spectra of the original and recovered **aPEG$_{10k}$** is shown in Figure S36 (bottom left).

Depolymerization and selective recovery of aPEG$_{10k}$ from mixed domestic wastes

Polyethylene, polypropylene, and aluminum foil were blended with 1 g of **aPEG$_{10k}$-1.2TREN** by hot press. The obtained polymer composite was then mixed with polyethylene, polypropylene, aluminum foil, tree bark, and leaves. Then, 15 mL of deionized H$_2$O was added to the solid mixture, which was kept at room temperature for 24 h (Figure S38, first line). The undissolved solids were filtered off and washed with water to completely recover the degraded chemicals. Next, 1 g of strongly acidic ion exchange resins was added to the filtrate, and the mixture was stirred for 30 min at room temperature. The resin was filtered off by vacuum filtration. The filtered solution was washed by activated carbon three times, and each time the suspensions were filtered by vacuum filtration. After the last filtration, the liquid phase was evaporated by rotary

evaporation. The residue, **aPEG₁₀ₖ**, was dried by vacuum drying at 70 °C for 24 h.

Recovered **aPEG₁₀ₖ**: 97.6 %, 965 mg. ^{1}H NMR (400 MHz, Chloroform-*d*) δ 4.33 – 4.30 (m, 2H), 3.73 (s, 2H), 3.66 (s, 459H), 3.50 (s, 2H), 2.29 (s, 3H).

The comparison between the ^{1}H NMR spectra of the original and recovered **aPEG₁₀ₖ** is shown in Figure S38 (bottom left).

Depolymerization and selective recovery of aPEG₁₀ₖ from commodity polymers

Polyvinyl chloride (**PVC**, Sigma Aldrich), polyethylene terephthalate (**PET**, Sigma Aldrich), polycarbonate (**PC**, Sigma Aldrich), and polystyrene (**PS**, Sigma Aldrich) were mixed with 1 g of **aPEG₁₀ₖ-1.2TREN**. Then, 15 mL of deionized H_2O was added to the solid mixture, which was kept at room temperature for 24 h (Figure S39, first line). The undissolved solids were filtered off and washed with water to completely recover the degraded chemicals. Next, 1 g of strongly acidic ion exchange resins was added to the filtrate, and the mixture was stirred for 30 min at room temperature. The resin was filtered off by vacuum filtration. The filtered solution was washed by activated carbon three times, and each time the suspensions were filtered by vacuum filtration. After the last filtration, the liquid phase was evaporated by rotary evaporation. The residue, **aPEG₁₀ₖ**, was dried by vacuum drying at 70 °C for 24 h.

Recovered **aPEG₁₀ₖ**: 96.9 %, 958 mg. ^{1}H NMR (400 MHz, Chloroform-*d*) δ 4.33 – 4.29 (m, 2H), 3.74 – 3.71 (m, 2H), 3.65 (s, 509H), 3.49 (s, 2H), 2.28 (s, 3H).

The comparison between the ^{1}H NMR spectra of the original and recovered **aPEG₁₀ₖ** is shown in Figure S39 (bottom left).
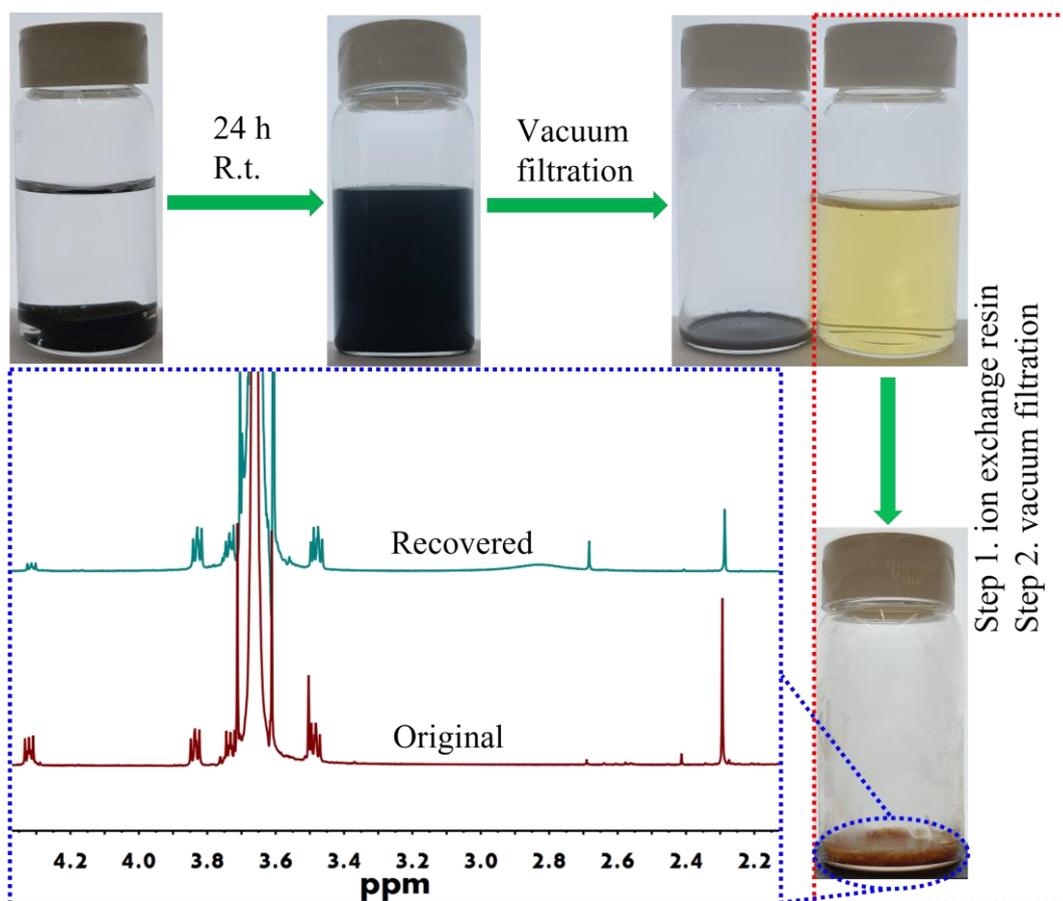
Figure S36. Photographs showing the depolymerization of **aPEG$_{10k}$-1.2TREN/MCNs**. The top left picture shows the initial state of 0.2 g **aPEG$_{10k}$-1.2TREN/MCNs** into 4 mL deionized water. After 24 h of depolymerization at room temperature, the polymer hydrolyzed and its components dissolved, while **MCNs** remained in suspension (top middle). The **MCNs** could be recovered by vacuum filtration (top right). The **aPEG$_{10k}$** obtained from the depolymerization process could be separated from **TREN** by treatment with ion exchange resins, followed by vacuum filtration (red dashed box). The comparison between the ^{1}H NMR spectra of the initial and recovered **aPEG$_{10k}$** is also shown.
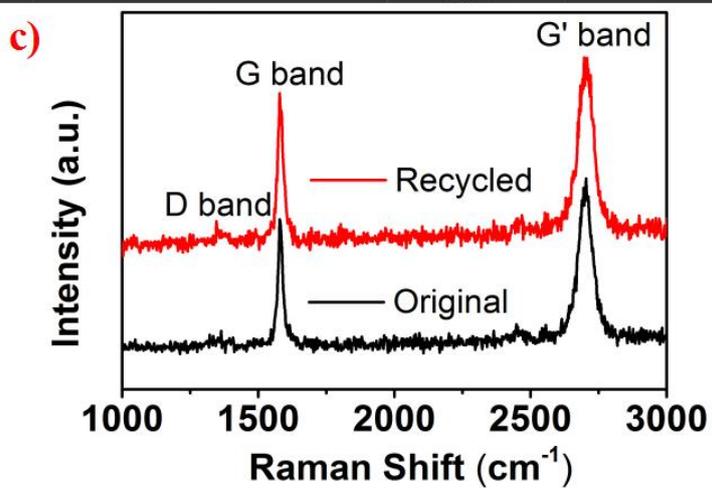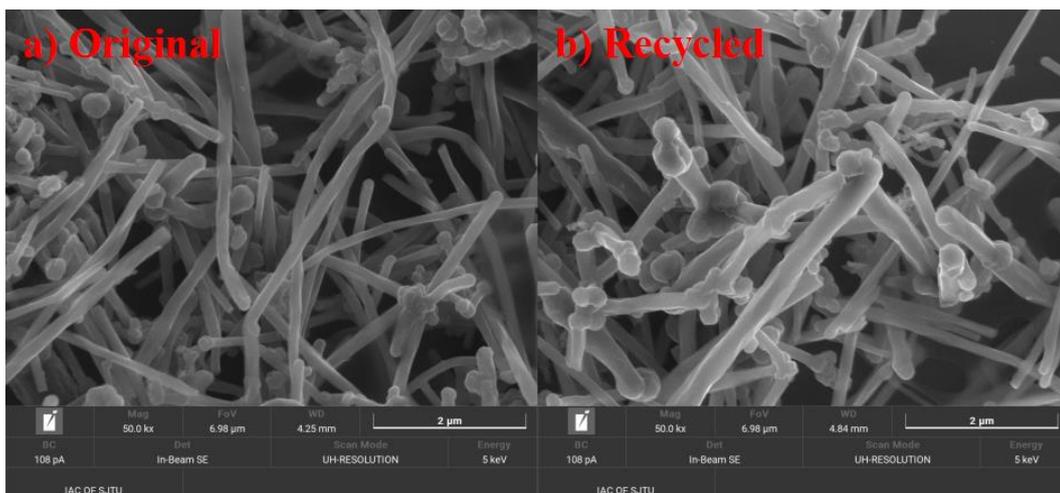
Figure S37. SEM images of the original (a) and recycled (b) **MCNs**. Overlaid Raman spectra of the original and recycled **MCNs** in the range of 1000-3000 cm^{-1} (c).
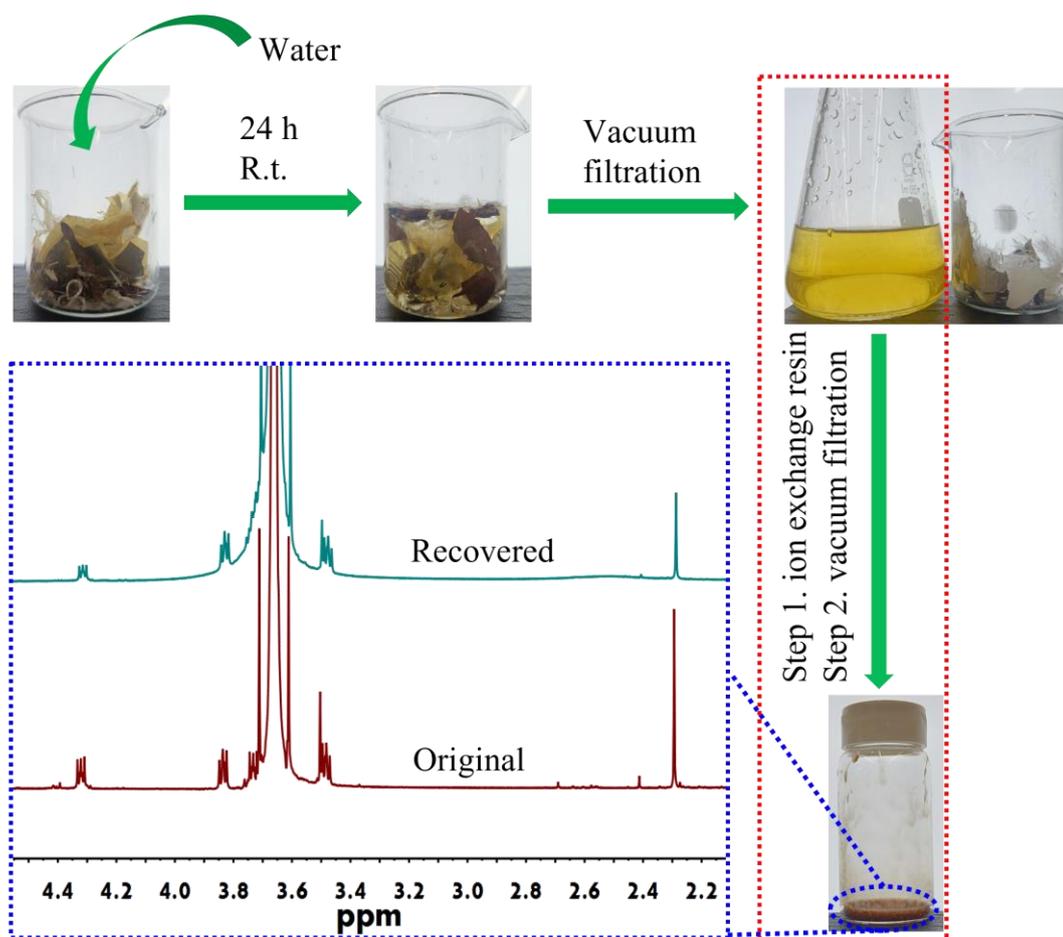
Figure S38. Photographs showing the depolymerization of **aPEG$_{10k}$-1.2TREN** containing various domestic wastes (polyethylene, polypropylene, aluminum foil, tree bark, and leaves). The top left picture shows the initial state of **aPEG$_{10k}$-1.2TREN** mixing or laminating or incorporating with various of domestic wastes. The top middle picture shows the initial state of the complex waste stream of the top left picture after the addition of 15 mL deionized water. After 24 h of depolymerization at room temperature, **aPEG$_{10k}$-1.2TREN** selectively hydrolyzed and its components dissolved, and the domestic wastes were filtered off by vacuum filtration (top right). The **aPEG$_{10k}$** obtained from the depolymerization process could be separated from **TREN** by treatment with ion exchange resins, followed by vacuum filtration (red dashed box). The comparison between the ^{1}H NMR spectra of the initial and recovered **aPEG$_{10k}$** is also shown.
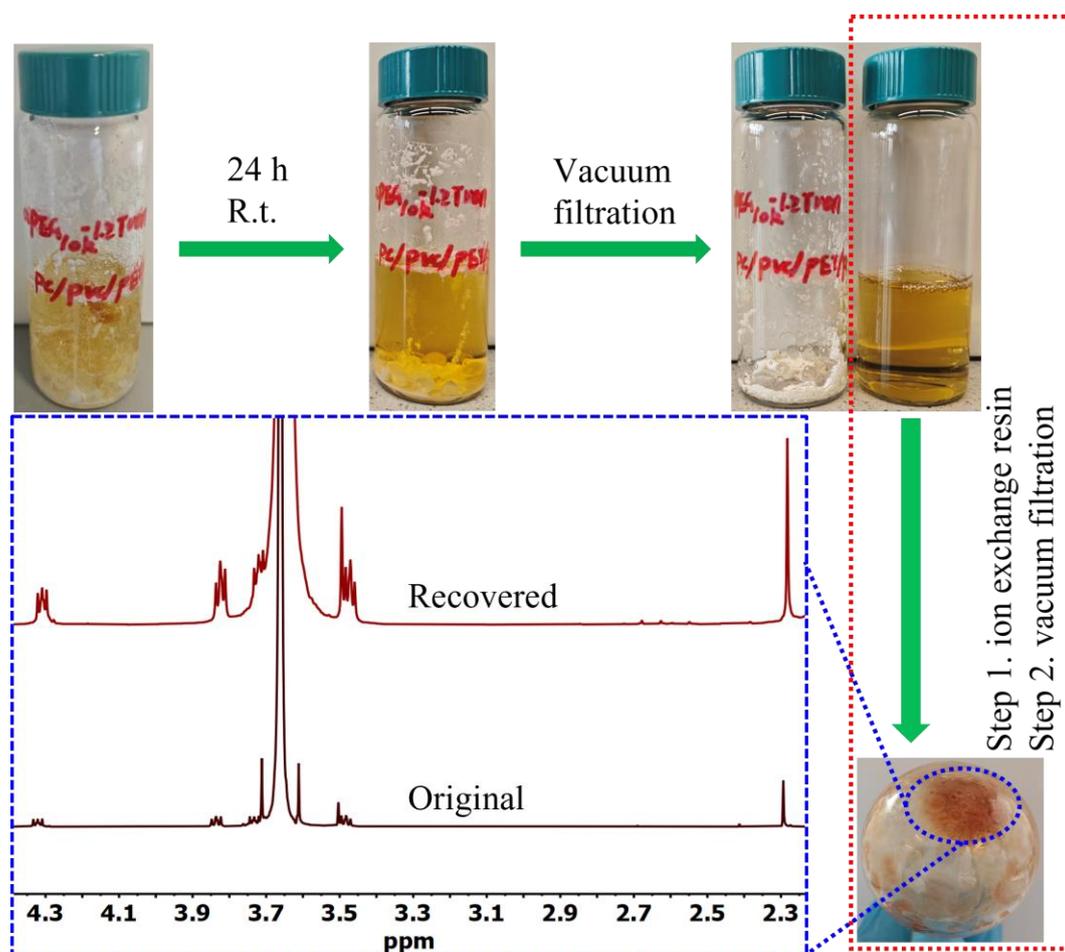
Figure S39. Photographs showing the depolymerization of **aPEG10k-1.2TREN** in the presence of various commodity polymers including polyvinyl chloride (**PVC**), polyethylene terephthalate (**PET**), polycarbonate (**PC**), and polystyrene (**PS**). The top left picture shows the initial state of **aPEG10k-1.2TREN** mixing with **PVC**, **PET**, **PC**, and **PS**. The top middle picture shows the initial state of the polymer mixture after the addition of 15 mL deionized water. After 24 h of depolymerization at room temperature, **aPEG10k-1.2TREN** selectively hydrolyzed and its components dissolved, and the commodity polymers were filtered off by vacuum filtration (top right). The **aPEG10k** obtained from the depolymerization process could be separated from **TREN** by treatment with ion exchange resins, followed by vacuum filtration (red dashed box). The comparison between the ^{1}H NMR spectra of the initial and recovered **aPEG10k** is also shown.

Reaction of aPEG$_{2k}$-Btl with benzylamine

Benzylamine (**Bzl**, 32.1 mg, 0.3 mmol) was added to a solution of **aPEG$_{2k}$-Btl** (110 mg, 0.05 mmol) in 3 mL of DMSO-d_6 in a 10 mL two-necked flask equipped with a stirring bar, under nitrogen. The mixture was heated (80, 100, or 120 °C) while stirring, and 0.5 mL of solution was taken out at different time intervals for ^{1}H NMR analysis (Figure S40). The reaction was followed by integration of the two ^{1}H NMR signals at 8.5 ppm and 8.8 pm assigned to the protons of -NH- for **aPEG$_{2k}$-Btl** and **aPEG$_{2k}$-Bzl** model compounds, respectively. The fraction of **aPEG$_{2k}$-Bzl** was calculated by integration of the ^{1}H NMR signals according to the equation:

Fraction **aPEG$_{2k}$-Bzl** = [**aPEG$_{2k}$-Bzl**]/[**aPEG$_{2k}$-Bzl** + **aPEG$_{2k}$-Btl**] = Integral of proton 2'/(Integral of proton 2' + Integral of proton 2).

Activation energies for the reaction of aPEG$_{2k}$-Btl with Bzl

The rate constants (k) for the reaction of **aPEG$_{2k}$-Btl** with **Bzl** were obtained by monitoring the fraction of **aPEG$_{2k}$-Bzl** in the reaction mixtures (Figure S41) under pseudo-first-order conditions (3 eq. **Bzl**) (Supplementary Equation 3). The activation energies ΔE for the reactions were determined by plotting $\ln(k)$ vs. T^{-1} (Supplementary Equation 2 at page S23).

Supplementary Equation (3):

$\ln$ (fraction **aPEG$_{2k}$-Bzl**) = -k(t), the fitting curves are shown in Figure S41.

The Arrhenius plot is shown in Figure S42, while the values obtained for k and the activation energy ΔE are shown in Table S6.
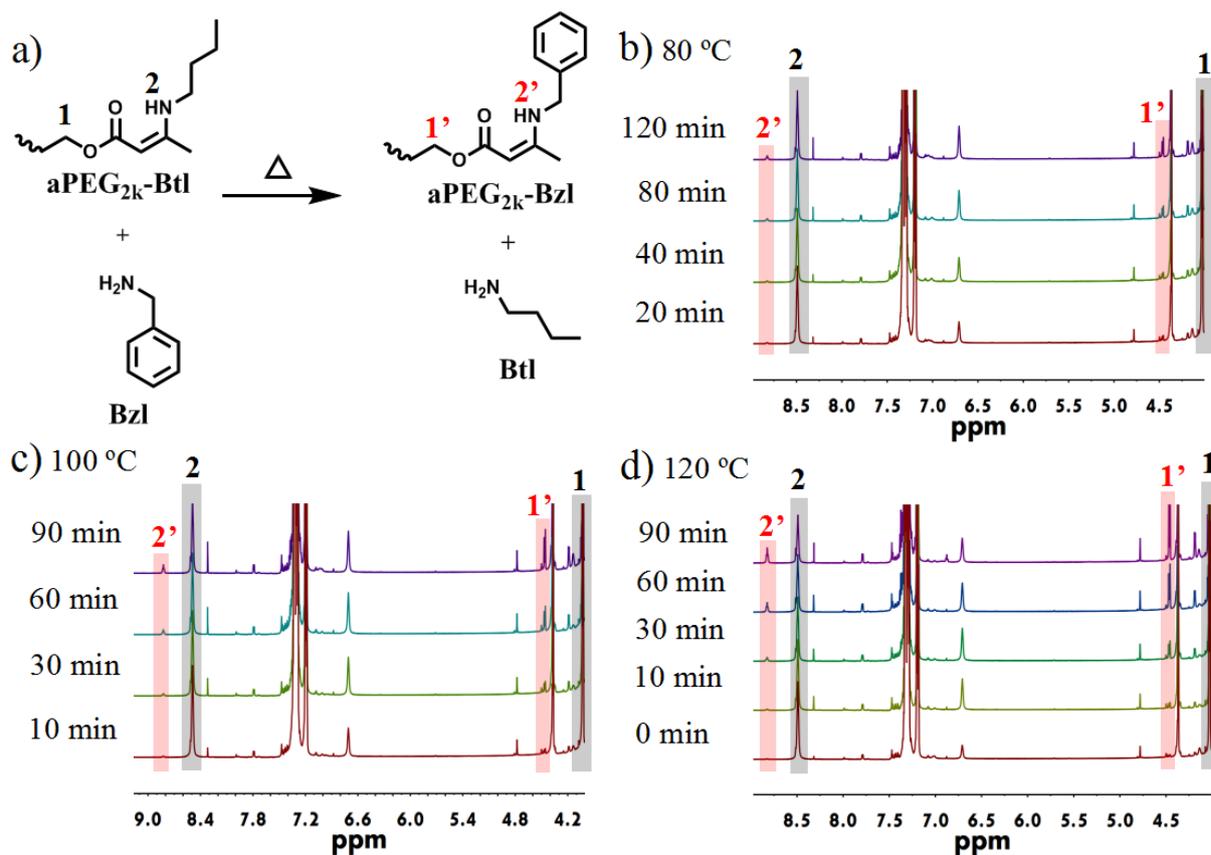
Figure S40. Scheme showing the conversion of **aPEG₂ₖ-Btl** and **Bzl** to **aPEG₂ₖ-Bzl** and **Btl**, and assignment of the protons used for the quantification of the conversion by integration of the ¹H NMR signals. Overlaid ¹H NMR spectra (DMSO-d_6, 700 MHz) depicting the shift of the protons **1** and **2** into **1'** and **2'** due to the transamination from **aPEG₂ₖ-Btl** into **aPEG₂ₖ-Bzl** at different reaction times (as indicated) at 80 °C, 100 °C and 120 °C.
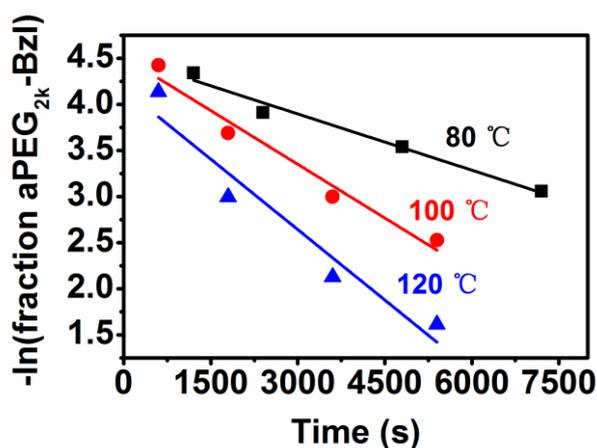

Figure S41. Fitting curves for the exchange reaction (transamination) involving **aPEG₂ₖ-Btl** and an excess of **Bzl** (3 eq.) at 80 °C (black), 100 °C (red), and 120 °C (blue).
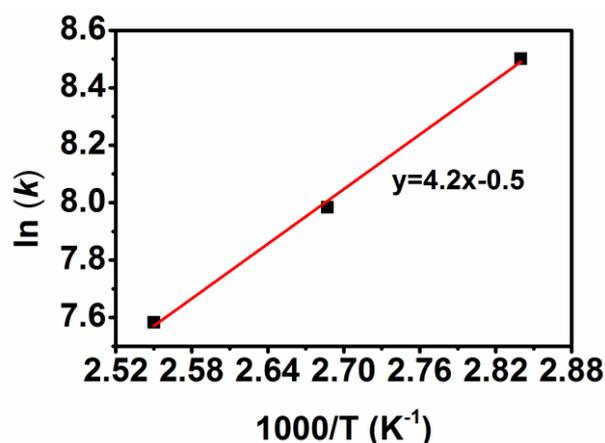
Figure S42. Arrhenius plot for the exchange reaction between **aPEG$_{2k}$-Btl** and an excess of **Bzl** (3 eq.), which provides an activation energy of 35 kJ mol^{-1}.

Table S6. Pseudo-first-order rate constants (k) and activation energy (E_a) for the hydrolysis between **aPEG$_{2k}$-Btl** and an excess of D$_2$O.

Temperature (°C)	Rate constants k (s^{-1})	Activation energy E_a (kJ mol^{-1})
80	2.0E-4	
100	3.9E-4	35
120	5.1E-4	

Activation energy for aPEG$_{2k}$-yTREN (y = 1.2, 1.5) network.

The activation energy was determined relying on the Maxwell model for stress-relaxation, according to Supplementary Equation (4):

$\sigma_t/\sigma_0 = \exp[-t/\tau]$,

where σ_t and σ_0 are the stress at time t and the initial stress, respectively, and τ is the relaxation time. By convention, the relaxation time is taken as the time at which the normalized stress is equal to 1/e (ca. 0.37).[28]

The obtained relaxation times (τ) measured at different temperatures (Figures S43a, S43c, Table S7) were fit to Supplementary Equation (5):

$\tau(T) = \tau_0 \times e^{E_a/RT}$

Supplementary Equation (5) can be transformed to Supplementary Equation (6):

$\ln\tau(T) = \ln\tau_0 + E_a/RT$

where R is the universal gas constant (8.31 J K^{-1} mol^{-1}), and T is the temperature expressed in Kelvin degrees.

The Arrhenius fits are shown in Figures S43(b), S43(d) and the calculated activation energy is shown in Table S7.

Topology freezing temperature (T_v) of aPEG$_{2k}$-yTREN (y = 1.2, 1.5) networks.

T_v corresponds to the freezing of network topology due to the absence of exchange reaction on the timescale of the observation, and it is usually defined as the temperature at which the melt viscosity is equal to 10^{12} Pa·s. Adopting the strategy from the Leibler group,[26] T_v could be calculated according to the Maxwell equation (Supplementary Equation 7):

$$\eta = G \times \tau(T_v)$$

Where G is the shear modulus and could be estimated from the storage modulus (E') as measured by DMA studies from Supplementary Equation (8):

$$G = E'/(2 (1 + v))$$

v is the Poisson's ratio and usually as 0.5, so Supplementary Equation (8) is transformed to Supplementary Equation (9):

$$G = E'/3$$

Here, E' is 0.8 MPa for **aPEG$_{2k}$-1.2TREN** and 1.6 MPa for **aPEG$_{2k}$-1.5TREN** at high temperatures. Thus, for **aPEG$_{2k}$-1.2TREN**, $\tau(T_v) = 10^{12}/(1/3 \times 0.8 \times 10^6) = 3.7 \times 10^6$ s. For **aPEG$_{2k}$-1.5TREN**, $\tau(T_v) = 10^{12}/(1/3 \times 1.6 \times 10^6) = 1.9 \times 10^6$ s. The relationship between temperature and stress relaxation time is shown in Supplementary Equation (5), then T_v is determined as the temperature for relaxation time of 3.7×10^6 s and 1.9×10^6 s, and the calculated T_v values are shown in Table S7.
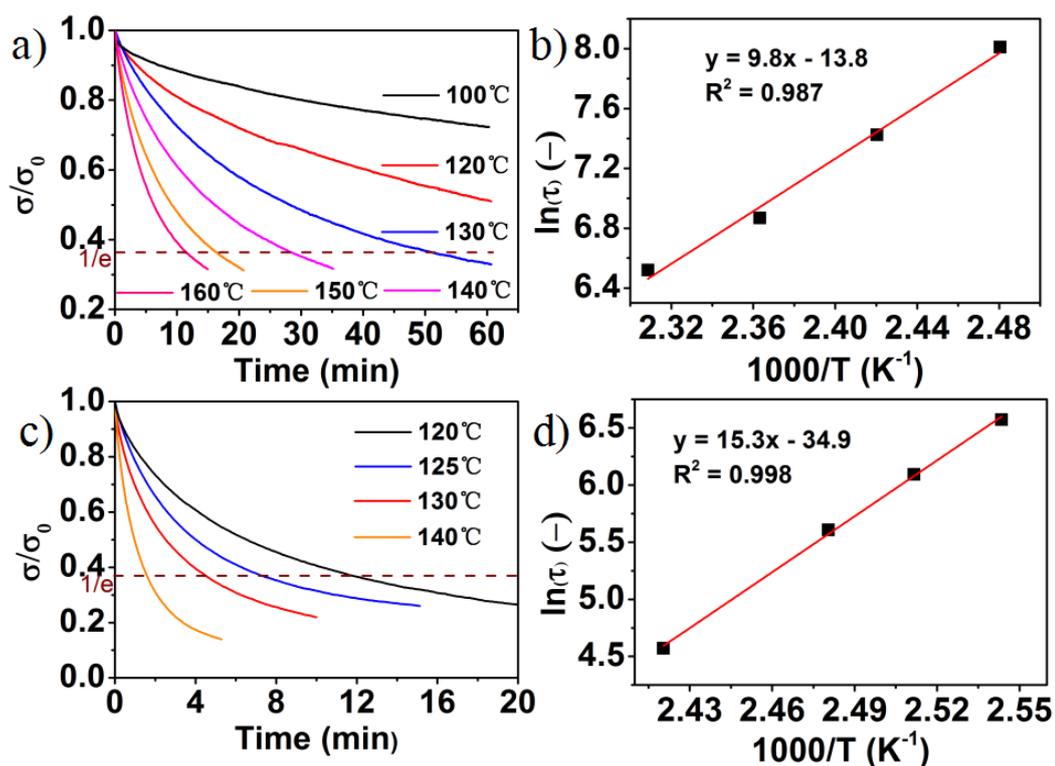
Figure S43. (a) Stress relaxation curves of **aPEG_{2k}-1.2TREN** measured as a function of time at 100 °C (black), 120 °C (red), 130 °C (blue), 140 °C (magenta), and 150 °C (orange), 160 °C (pink), and (b) related Arrhenius plots for the stress-relaxation. The calculated activation energy is 81.4 kJ mol^{-1}. (c) Stress relaxation curves of **aPEG_{2k}-1.5TREN** measured as a function of time at 120 °C (black), 125 °C (blue), 130 °C (red), and 140 °C (orange), and (d) related Arrhenius plots for the stress-relaxation. The calculated activation energy is 127.1 kJ mol^{-1}.

Table S7. Summary of the stress relaxation times at different temperatures $\tau(T)$, activation energies E_a, and topology freezing temperature T_v of **aPEG₂ₖ-yTREN** (**y** = 1.2, 1.5).

| Sample name	Temperature (°C)	Relaxation times (s)	Arrhenius fitting equations; Activation energies (kJ mol^{-1})	Topology freezing temperature (°C)
aPEG₂ₖ-1.2TREN	130	3008	y = 9.8x-13.8, R^2 = 99%; 81.4	66
	140	1676		
	150	962		
	160	678		
aPEG₂ₖ-1.5TREN	120	714	y = 15.3x-34.9, R^2 = 99%; 127.1	40
	125	443		
	130	273		
	140	97		
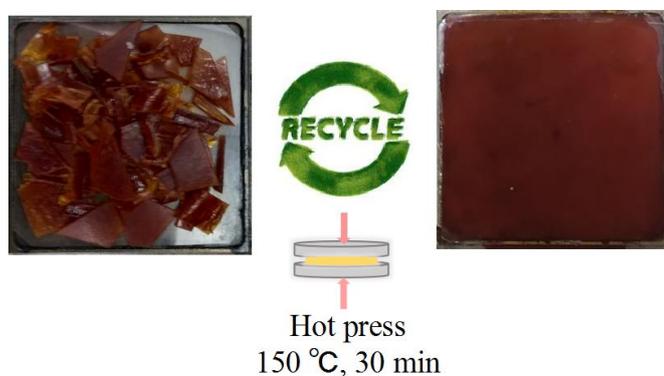
Figure S44. Thermal reprocessing of **aPEG₂ₖ-1.2TREN** from small pieces of material (left) into a new film (right) by hot press (T = 150 °C; P = 10 MPa; time = 30 min).

References

[18] Y. Lin, Y. Chen, Z. Yu, Z. Huang, J. Lai, J. B.-H. Tok, Y. Cui, Z. Bao, *Chem. Mater.*, 2022, 34, 2393-2399.

[26] M. Capelot, M. M. Unterlass, F. Tournilhac, L. Leibler, *ACS Macro Lett.*, 2012, 1, 789-792.

[27] B. Wunderlich, *Macromolecular Physics - Crystal Melting*, Academic Press, Inc., New York, NY, 1980.

[28] Z. Liu, C. Yu, C. Zhang, Z. Shi, J. Yin, *ACS Macro Lett.*, 2019, 8, 233-238.